EMORY
UNIVERSITY
SCHOOL OF
MEDICINE

THE INAUGURAL EMORY PHYSICIAN SCIENTIST *Symposium*

MAY 17, 2024

NEW LOCATION
HSRB I & II

NIH National Heart, Lung, and Blood Institute

R38HL167243

Contents

Don't forget to vote for Best Poster!

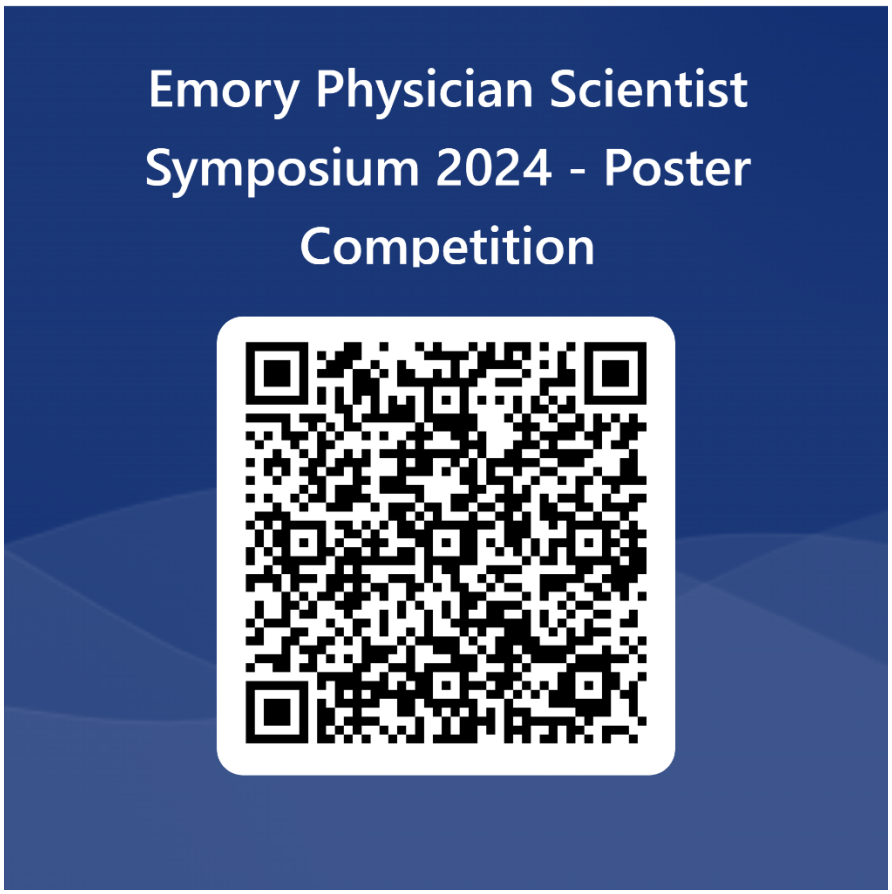

Oral Presentation Abstracts

Listed in Alphabetical Order by Presenting Author

Valerobetaine is a Microbe-Generated Metabolite that Impacts Epithelial Barrier Integrity in the Colon

Presenting Author: Askew, Lauren, BS, Pediatrics

Askew, Lauren; Gacasan, Anthony; Barbian, Stefi; Jones, Rheinallt.

Background: The gut microbiome generates bioactive small molecules and metabolites that impact gut physiology. Recent investigations have focused on identifying the molecular mechanisms through which these gut microbiota-generated metabolites function. Utilizing germ-free mice and mass spectrometry-based metabolomics for analysis of small molecules, our research group demonstrated distinct differences in the metabolome of the liver between germ-free and conventional mice. The most discriminatory metabolite generated by the gut microbiome was δ-valerobetaine (VB). Our previous studies showed that VB suppresses mitochondrial fatty acid oxidation in hepatic cells by decreasing cellular carnitine levels. We showed that VB is a central integrator through which the microbiota influences energy metabolism in the liver. However, little is known about how VB may impact gut physiology. To this end, our initial studies have shown that VB induces mitochondrial biogenesis within ileal crypts. Hypothesis: Through its effect on mitochondrial bioenergetics, VB promotes gut epithelial barrier integrity and intestinal cell homeostasis. Methods: Conventional mice were treated intraperitoneally with 50mg/kg VB or vehicle control. Upon sacrifice, the colon was harvested and analyzed to assess if VB impacts the expression of genes that function in gut epithelial barrier integrity. Cultured human colonic cell monolayers were grown to confluency and scratched to simulate a wound. VB was administered to the media and wound closure rate followed. In addition, the expression of genes that function in gut epithelial integrity was measured in cultured colonic cells treated with VB. To assess barrier integrity, cells were grown on Transwell inserts, treated with VB, and the trans-epithelial electrical resistance (TEER) measured. Results: Germ-free mice treated with VB exhibited lower gene expression of Claudin 1, 2, and 3, but higher expression of Claudin 4. These changes in claudin expression were also corroborated in cultured colonic cells. VB treatment significantly increased wound closure rates, and increased barrier integrity in cultured cells at 48hrs following treatment. Conclusions: Our results show that the microbiome generated metabolite, VB, is a modulator of epithelial barrier integrity, thereby implicating VB as an integrator of host cell and microbe interactions in the gut epithelium.

Compliance Diem: Seize the Evidence for Emergency CT Evaluation of Pediatric Seizures

Presenting Author: Bechel, M, MD PhD, Radiology

Bechel, M; Lin, Jenny; Jain, Shobhit; Allen, Kelsey; and Reddy, Kartik.

Background: In the absence of head trauma and VP shunts, head CT in children with seizures has little diagnostic utility. Children's Healthcare of Atlanta (CHOA) ED had implemented a local guideline for imaging for seizures, but discontinued its use in 2016. The objectives of this study are to evaluate: 1) appropriateness of head CT use in the absence of local guidelines and 2) drivers of head CT use in seizure.

Methods: Retrospective chart review examining patients presenting to a CHOA ED for seizure between May 1, 2022 and May 31, 2023. Using natural language processing, we evaluated the appropriateness of head CT imaging for these patients according to three imaging guidelines (CHOA ED guideline, American Academy of Neurology (AAN), and American College of Radiology (ACR)). Using feedforward logistic regression, we evaluated patient, clinician, and system factors for association with head CT use.

Results: Of the 1426 patients presenting to the ED for seizure, 113 (7.9%) had head or facial trauma, 150 (10.5%) had VP shunts, and 1153 (80.8%) had a history of prior seizures. By the CHOA, AAN, and ACR guidelines, 319 (22.3%), 394 (27.6%), and 133 (9.3%) patients would have qualified for imaging respectively. Of those 137 (9.6%) that received a head CT in the ED, 62 (45%) met the CHOA guideline and 33 (24.1%) met no guideline at all. The most predictive factors for imaging included: number of guidelines met ($p<0.0001$), subsequent admission ($p<0.0001$), first seizure ($p<0.001$), and head trauma ($p=0.03$). Notable factors not associated with imaging include: high risk population, repeat ED visits, neurology consult, and time of day. During the study period, 5520 head CTs were ordered from the ED and 610 (11%) had 'seizure' or 'epilepsy' in the indication. 129 (21.2%) had presented with seizure.

Conclusions: Six years after discontinuation, compliance to the CHOA guideline persists, beyond that of other national guidelines. Yet, about a quarter of patients meet no criteria for imaging and 79% of ED head CT orders for 'seizure' are not associated with clinical seizures. This disconnect indicates a considerable opportunity for improvement of the collaboration between the ED and radiology.

Redefining Diagnostic Lesional Status in Temporal Lobe Epilepsy with Artificial Intelligence

Presenting Author: Gleichgerrcht, Ezequiel, MD, PhD, Neurology

GLEICHGERRCHT, EZEQUIEL; Kaestner, Erik; Hassanzadeh, Reihaneh; Roth, Rebecca W.; Parashos, Alexandra; Davis, Kathryn A.; Bagić, A; Keller, Simon S.; Rüber, Theodor; Stoub, Travis; Pardoe, Heath R.; Dugan, Patricia; Drane, Daniel L.; Abrol, Anees; Calhoun, Vince; Kuzniecky, Ruben I.; McDonald, Carrie R.; Bonilha, Leonardo.

Background: Despite decades of advancements in diagnostic MRI, 30-50% of temporal lobe epilepsy (TLE) patients remain categorized as "non-lesional" (i.e., MRI negative or MRI–) based on visual assessment by human experts. MRI– patients face diagnostic uncertainty and significant delays in treatment planning. Quantitative MRI studies have demonstrated that MRI– patients often exhibit a TLE-specific pattern of temporal and limbic atrophy that may be too subtle for the human eye to

detect. This signature pattern could be successfully translated into clinical use via artificial intelligence (AI) advances in computer-aided MRI interpretation, thereby improving the detection of brain "lesional" patterns associated with TLE.

Methods: Here, we tested this hypothesis by employing a three-dimensional convolutional neural network (3D CNN) applied to a dataset of 1,178 scans from 12 different centers. 3D CNN was able to differentiate TLE from healthy controls with high accuracy (85.9% ± 2.8), significantly outperforming support vector machines based on hippocampal (74.4% ± 2.6) and whole-brain (78.3% ± 3.3) volumes.

Results: Our analysis subsequently focused on a subset of patients who achieved sustained seizure freedom post-surgery as a gold standard for confirming TLE. Importantly, MRI– patients from this cohort were accurately identified as TLE 82.7% ± 0.9 of the time, an encouraging finding since clinically these were all patients considered to be MRI– (i.e., not radiographically different than controls). The saliency maps from the CNN revealed that limbic structures, particularly medial temporal, cingulate, and orbitofrontal areas, were most influential in classification, confirming the importance of the well-established TLE signature atrophy pattern for diagnosis. Indeed, the saliency maps were similar in MRI+ and MRI– TLE groups

Conclusions: Our results suggest that even when humans cannot distinguish more subtle levels of atrophy, MRI– patients are on the same continuum common across all TLE patients. As such, AI can identify TLE lesional patterns and AI-aided diagnosis has the potential to greatly enhance the neuroimaging diagnosis of TLE and redefine the concept of "lesional"

VIPR Antagonism Drives Metabolically Fit, Memory-Rich CAR T Cells for the Treatment of Pancreatic Cancer

Presenting Author: Lin, Heather, BS, MSTP School of Medicine

LIN, HEATHER; Blake, Dejah; Wells, Kory; Mudigonda, Abhijay; Liu, William; Evans, Alysa; Goyal, Subir; Liu, Tongrui; Freeman, Ruby; Funk, Christopher; Sinha, Tanisha; Christensen, Elyse; Mahmood, Naeman; Fei, Fan; Heller, Brad; Chun, Paul; Passang, Tenzin; Ravindranathan, Sruthi; Dougan, Jodi; Porter, Christopher; Patgiri, Anupam; Yang, Lily; Waller, Edmund; and Rafiq, Sarwish.

Background: Chimeric antigen receptor (CAR) T therapies for pancreatic ductal adenocarcinoma (PDAC) still face significant immunosuppressive obstacles in the tumor microenvironment (TME). An optimal CAR T cell for PDAC combines targeting an ideal tumor-associated antigen and overcomes the immunosuppressive microenvironemnt of PDAC. The retained ectodomain of Muc16 (Muc16CD) has yet to be explored in PDAC. Vasoactive intestinal peptide (VIP) is an emerging checkpoint pathway of T cell function abundantly expressed by PDAC. In this work, we present a novel armored CAR T cell that targets Muc16CD and antagonizes VIPRs (CAR/VIPRa) to overcome the immunosuppressive PDAC TME.

Methods: Patient data was generated by the TCGA Research Network. Primary human T cells from healthy donors or PDAC patients were retrovirally transduced to express Muc16CD-directed CARs with or without secretion of novel, potent VIPR antagonist peptides.

Results: PDAC tumors have significantly increased expression of Muc16 compared to normal pancreas tissue and patients with high Muc16 expression have a significantly decreased overall survival. PDAC patient-derived tumors show robust expression of both Muc16CD and VIP. CAR/VIPRa T cells reveal that VIPR antagonism metabolically reprograms CAR T cells and drives a memory-rich product. CAR/VIPRa T cells are less activated and less exhausted by the manufacturing process, which lends to better viability and a metabolically quiescent phenotype at baseline. These distinct features allow CAR/VIPRa T cells, when antigen-stimulated, to have enhanced effector functions. To investigate clinical relevance, CAR/VIPRa T cells manufactured from PDAC patient blood also significantly enrich memory phenotypes. In vivo, CAR/VIPRa T cells have enhanced expansion, phenotype, infiltration, and persistence, which significantly reduces PDAC tumor burden. In patient-derived PDAC preclinical mouse models where CAR T is typically ineffective, CAR/VIPRa T cells significantly reduce tumor burden.

Conclusions: This work demonstrates Muc16CD and VIP as a clinically relevant targets for CAR T therapy in PDAC. Collectively, this data demonstrates that novel CAR/VIPRa T cells create an advantageous cellular therapy product capable of treating PDAC. The long-term goal of this work is translating CAR/VIPRa T cells for the treatment of PDAC and expanding these preclinical findings of cellular therapies for other VIP-abundant tumors.

Development of a Novel L-Asparaginase with Reduced Toxicity Utilizing Ancestral Sequence Reconstruction

Presenting Author: Raikar, Sunil, MD, Pediatrics

Knight, Kristopher; Brown, Harrison; White, Kinnede; Spencer, H. Trent; Doering, Christopher and RAIKAR, SUNIL.

Background: L-asparaginase (L-ASNase) has been a critical component of acute lymphoblastic leukemia (ALL) chemotherapy regimens for several decades. Current clinical L-ASNases are bacterial in origin and thus highly immunogenic. Additionally, significant liver and pancreatic toxicity can be seen due to the glutaminase co-activity in bacterial L-ASNases. Thus, development of a less immunogenic L-ASNase with reduced glutaminase activity is essential to overcome its limitations. The anti-tumor properties of L-ASNase were first discovered serendipitously in guinea pig (GP) L-ASNase. GP L-ASNase has significantly favorable anti-leukemic and enzyme kinetics compared to human L-ASNase. It shares ~70% sequence identity with human L-ASNase compared to ~30% by bacterial L-ASNases and has no glutaminase co-activity. Thus, GP L-ASNase serves as the ideal template to create a humanized, less toxic L-ASNase. Ancestral Sequence Reconstruction (ASR) is an innovative protein drug optimization platform that can be leveraged to improve pharmaceutical properties of L-

ASNase. Analysis of the predicted molecular evolution of L-ASNase maps the functional divergence of extant orthologs by means of evolutionary intermediaries, enabling identification of critical residues responsible for superior activity.

Methods: ASR was performed utilizing 54 extant L- ASNase sequences. 53 ancestral L-ASNase (An-ASNase) sequences were identified and ten variants spanning the human and GP lineage were resurrected. E.coli codon optimized cDNA sequences were subcloned into an expression vector and transformed into E.coli BL21(DE3) cells for protein expression. An-ASNase candidates were isolated through Ni2+ affinity chromatography. L-ASNase activity was assessed using a modified Nessler's reagent assay.

Results: At an enzyme concentration of 0.1 mg/mL and an asparagine substrate concentration of 1 µM, An-88, An-104, and An-107 exhibited outstanding L-ASNase activity, comparable to clinically relevant E.coli and Erwinia L-ASNases. An-88 has 81% similarity, while both An-104 and An-107 ASNases shared an 88% identity with human L-ASNase. Preliminary cytotoxicity assessments of An-104 and An-107 on a T-ALL cell line, CCRF-CEM, demonstrated comparable anti-leukemia cytotoxicity to existing bacterial L-ASNases, with An-107 demonstrating the highest cytotoxicity.

Conclusions: We have shown that ASR is a viable platform to bioengineer a less toxic humanized L-ASNase drug candidate. Lead candidate toxicity profile will be defined, and chemotherapeutic potential will be measured against ALL.

The CD8+ T Cell Landscape of Human Brain Metastases

Presenting Author: Sudmeier, Lisa, MD, PhD, Radiation Oncology

SUDMEIER, LISA; Hoang, Kimberly; Nduom, Edjah; Wieland, Andreas; Neill, Stewart; Schniederjan, Matthew; Ramalingam, Suresh; Olson, Jeffrey; Ahmed, Rafi; Hudson, William.

Brain metastases are the most common adult brain tumor and are associated with poor overall survival and significant neurological morbidity. Immunotherapy, specifically immune checkpoint inhibitors (ICI) that target inhibitory molecules like PD-1 on CD8+ T cells, have demonstrated significant efficacy in the treatment of numerous cancer types; their use in the last decade has reshaped the way many cancers are treated. While there is a signal for ICI efficacy in the brain, patients with brain metastases continue to suffer poor overall survival rates in the ICI era. This may, in part, be due to the unique immune environment of the brain, which evolved to tightly regulate and restrict inflammatory processes that are known to cause neurodegenerative conditions. In order to develop more effective immunotherapeutic strategies for the treatment of brain metastases, it is critical to understand the interplay between the brain microenvironment and the tumor immune microenvironment. In the work presented here, we focus on characterizing the phenotype of brain metastasis infiltrating CD8+ T cells. Human brain metastases samples were received at the time of surgical resection with matched peripheral blood samples. Immune cells were isolated, and CD8+ T cells were phenotyped by flow cytometry and single-cell RNA sequencing with T cell receptor (VDJ)

sequencing. Spatial organization of the brain metastasis immune microenvironment was characterized with spatial transcriptomics. We show that brain metastases are infiltrated by populations of phenotypically distinct CD8+T cells, many of which express PD-1. CD8+ T cells appear to be differentiating within the brain metastasis microenvironment based on clonal overlap between the proliferating and functionally exhausted CD8+ T cell populations. Bystander CD8+ T cells specific for microbial antigens also infiltrate human brain metastases and are largely confined to the phenotypically less exhausted CD8+ T cell populations in the tumor. The different populations of CD8+ T cells occupy discrete spatial niches within the brain metastasis microenvironment. Our work suggests that signaling pathways within these niches should be investigated further as potential targets to improve the efficacy of immunotherapy for the treatment of brain metastases.

IgM Antibodies in ALS: Further evidence for immune activation in ALS

Presenting Author: Thomas, Eleanor, MD/PhD, Neurology

Thomas, Eleanor V.; McEachin, Zachary T.; Dammer, Eric B.; Trautwig, Adam; Assefa, Ezana; Asress, Seneshaw; Jiang, Jie; Seyfried, Nicholas T. ; and Glass, Jonathan D..

OBJECTIVE: To investigate immune mechanisms of ALS disease progression

BACKGROUND: Neuroinflammation is increasingly recognized as an important disease mechanism in ALS. Previous work has demonstrated differences in T and B cell populations in ALS patients that contribute towards disease progression.

METHODS: We performed a proteomic search of motor cortex and CSF for markers of ALS pathogenesis. Further validation of proteomic results was performed via immunoblot and immunohistochemistry (IHC).

RESULTS: We identified a remarkable upregulation of proteins associated with IgM immune complexes using unbiased tandem-mass-tag (TMT) mass-spectrometry proteomics from 18 sALS, 17 c9ALS, and 17 controls. Immunoglobulin heavy constant mu (IGHM) and its J (joining) chain were upregulated in both sALS and c9ALS motor cortex. An analysis of CSF from 29 sALS, 10 c9ALS, and 44 healthy controls again demonstrated elevated IGHM and J Chain in c9ALS. To further investigate the etiology for elevated IgM in ALS patient CNS tissues immunoblotting and IHC were performed from c9ALS, sALS and control motor cortex. Immunoblotting confirmed elevated IGHM in sALS and c9ALS motor cortex, and IHC from these samples demonstrate IGHM deposition associated with blood vessels and markers for neurons and astrocytes. Further experiments are being performed to identify IgM antigens in ALS brain by immunoprecipitation of IgM immune complexes followed by mass spectrometry-based proteomic analysis.

CONCLUSION: Since both the secretory J chain and IgM heavy chain, were elevated in ALS motor cortex and CSF, it points to the presence of IgM pentamers, which are large ~900 kDa macromolecular complexes with 10 antigen bindings sites. We hypothesize that disruption of the

blood brain barrier (BBB) in ALS may lead to exposure of CNS antigens to the peripheral immune system resulting in a loss of tolerance and the development of autoreactive IgM antibodies in ALS.

Inducible costimulatory molecule is important in the efficacy of Th17 Therapy

Presenting Author: Wittling, Megen, Bachelor of Science in Biology from Georgia Tech, Cancer Biology

WITTLING, MEGEN; and Knochelmann, Hannah; and Kumarasan, Soundharya; and Wyatt, Megan; and Cole, Anna; and Bennett, Frances; and Swisher, Shannon; and Paulos, Chrystal.

Background: Adoptive T cell therapy is a very promising approach for the treatment of cancer, with many FDA-approved CAR T cell therapies for hematologic malignancies as well as improving success for solid tumors. Due to the need to continue to optimize these treatments for patients with hard-to-treat tumors, our lab has developed a model in which we can study adoptive T cell therapy for melanoma. We have found that antigen specific Th17 cells are potent regressors of melanoma tumors in our mice model and regress melanoma better than Th1 and other CD4 subsets. Due to the high expression of Inducible Costimulatory Molecule (ICOS) on these cells, I wanted to explore the role of ICOS in this therapy.

Methods: Antigen-specific TRP-1 CD4+ T cells were polarized to the Th17 phenotype and were adoptively transferred into B16F10 melanoma bearing mice. ICOS signaling was then diminished by either antibody blockade or genetic deletion and compared to mice given an isotype control. RNA-Sequencing, flow cytometry, and tumor growth measurements were additionally used to assess differences when ICOS was blocked or not.

Results: ICOS was found to be important in the success of Th17 therapy for the treatment of melanoma as when blocking this costimulatory pathway, both survival and antitumor activity was negatively impacted. Additionally, this signaling pathway appears to be important early on after Th17 cell transfer into mice as blocking this pathway early on but not at later time points compromised antitumor immunity. I also assessed which cells express the binding partner to ICOS (ICOS-Ligand), which has important implications for therapeutic success.

Conclusions: The costimulatory molecule ICOS has an important role for the antitumor activity of Th17 cell therapy targeting melanoma.

Poster Competition Abstracts

Listed in Alphabetical Order by Presenting Author

Multi-institutional Analysis of Choledocholithiasis in Pediatric vs Adult Patients: Taking Back the Duct

Presenting Author: Aworanti, Eunice, MS, Emory University School of Medicine, Pediatric Surgery

Poster Number: 1

Dantes G; Rauh JL; Smith SR; AWORANTI, EUNICE; Wallace M; Collings A; Sanin, GD; Cambronero GE; Bosley ME; Ignacio R; Knod JL; Slater B; Callier K; Livingston MH; Dukleska K; Scholz S; Zamora IJ; Clifton, M; Knauer EM; Santore M; H Alemayehu; Neff LP

Background: The burden of choledocholithiasis is not limited to adult patients as the incidence of biliary disease has increased in children. With adult patients, the use of intraoperative cholangiogram (IOC) alongside laparoscopic common bile duct exploration (LCBDE) is widely accepted; however, the perceived intricacy of LCBDE, compounded by the unique challenges of pediatric anatomy and a scarcity of comparative data, has impeded the widespread adoption of this "surgery first" strategy in the pediatric population. To explore this, we utilized a multicenter collaborative to compare the success rates of LCBDE between adult and pediatric patients.

Methods: A multicenter, retrospective review of pediatric (<18 years old) and adult patients with suspected choledocholithiasis managed from 2018-2022 was performed. Demographic and clinical data were obtained. Our primary outcome was rate of successful duct clearance with upfront LCBDE. Operative fluoroscopy time, outcomes, and complications (infections, bleeding, pancreatitis, bile leak) were also compared.

Results: 333 (45.9%) pediatric and 391 (54.0%) adult patients were evaluated. The median age of pediatric vs adult patients was 15.2 vs 55.5 years, respectively. IOC was performed in 178 (53.5%) pediatric and 166 (42.5%) adult patients (p=0.003). Eighty-four (25.2%) pediatric vs 140 (35.8%) adults patients underwent LCBDE (p=0.002). LCBDE success was no different between pediatric and adult patients (85.7% vs 76.4%, p=0.12) respectively. ERCP was performed prior to laparoscopic cholecystectomy in 132 (39.6%) pediatric vs 222 (56.8%) adult patients (p=0.984). Four (3.03%) vs 7 (3.15%) pediatric vs adult patients required LCBDE following ERCP, p=1.00. Surgical complications were similar in pediatric vs adult patients (3.0% vs 3.8%, p=0.68).

Conclusion: In conclusion, our multicenter collaborative study comparing the management of choledocholithiasis in pediatric and adult patients reveals that LCBDE is similarly successful in adult and pediatric cohorts with no difference in surgical complications. These findings support the consideration of the use of intraoperative cholangiogram (IOC) alongside laparoscopic common bile duct exploration (LCBDE) in management of choledocholithiasis among both populations. As access to ERCP is limited, continued training, education, and dissemination of LCBDE techniques is necessary.

Butyrate Supplementation During Pregnancy Reduces Injury in Murine Model of Neonatal Intestinal Inflammation

Presenting Author: Barbian, Maria, MD, Pediatrics

Poster Number: 2

BARBIAN, MARIA; Naudin, Crystal; Denning, Patricia, Patel, Ravi; and Jones, Rheinallt

Background: The diet during pregnancy (antenatal diet) [PRM1] impacts fetal gut development. Butyrate is a short-chain fatty acid (SCFA), generated by gut bacteria, which dampens gut inflammation. Previously, we demonstrated that antenatal butyrate supplementation (ABS) in mice reduces intestinal injury from experimentally-induced colitis in adult murine offspring.

Objective: Evaluate whether ABS reduces intestinal injury in a murine model of neonatal intestinal inflammation. We hypothesize that ABS will reduce intestinal injury in neonatal offspring exposed to intestinal inflammation via down regulation of inflammation.

Methods: Breeding pairs of C57BL/6 mice were assigned to control or ABS group. ABS mice received 90mM of sodium butyrate in their drinking water during pregnancy, while pregnant control mice did not receive any butyrate supplementation. To assess the influence of ABS on the prenatal versus postnatal environment, a cross fostering model was also employed. Next, two-week-old offspring underwent an established model of neonatal gut injury through intraperitoneal injection of lipopolysaccharide and platelet activating factor. Gut injury was measured through blinded histopathologic scoring. Samples of maternal stool, colon, amniotic fluid, breast milk, neonatal colon and stool and fetal gut were collected for SCFA analysis via gas chromatography mass spectrometry.

Results: Gut histopathologic scoring revealed ABS offspring have less injury than control offspring ($P=0.02$). Through RT-qPCR from ileum tissue samples, ABS offspring had 3.5-times higher levels of TGF-β1 mRNA expression ($P=0.02$) and 90-times lower NF-κB expression ($P=0.04$). Cross-fostering model suggests that ABS may reduce injury in neonatal offspring through changes in the postnatal environment. SCFA analysis revealed high butyrate content in breast milk from ABS dams ($p = 0.003$).

Conclusions: Butyrate supplementation during pregnancy resulted in reduced intestinal injury in neonatal murine offspring. This may be secondary to decreased inflammatory tone in the intestine of the offspring, given increases in TGF-β1 and decreases in NF-κB signaling. From our preliminary findings, ABS may protect against intestinal injury in neonatal offspring through influence on the postnatal environment, such as breast milk butyrate content. Thus, ABS may protect against gut injury through elevated butyrate in maternal milk leading to lower gut inflammation.

Functional Differences in Circulating versus Tumor Infiltrating CD27/28- CD57+ T cells Isolated from Head and Neck Squamous Cell Cancer Patients

Presenting Author: Brammer, Brianna, BS, School of Medicine

Poster Number: 3

BRAMMER, BRIANNA; Kinney, Brendan; Kansal, Vikash; and Schmitt, Nicole

Background: Approximately half of patients with head and neck squamous cell carcinoma (HNSCC) will experience disease recurrence within one year after standardized therapy. Although HNSCC development is well associated with carcinogen exposure (tobacco, alcohol) and high-risk human papillomavirus (HPV) strains, many patients have no known risk factors beyond increased age. A possible emerging risk factor exists in a subset of T cells characterized by loss of co-stimulatory molecules CD27/28 and expression of CD57, which develop in response to chronic antigen stimulation; we refer to these CD27/28- CD57+ T cells as HD TEMRA cells. Prognostic studies have yielded mixed results on the impact of HD TEMRA cells, even within the same tumor type. There is an unmet need to determine the functional phenotype of HD TEMRA cells in HPV- HNSCC to understand their true prognostic association.

Methods: We are performing on-going prognostic studies in our surgically treated HPV- HNSCC patient cohort. Utilizing matched HNSCC patient blood and tumor samples, we determined relative quantities of HD TEMRA cells, and performed functional assays to characterize HD TEMRA activation markers, proliferation, and cytokine production.

Results: In our initial cohort study, we found that HPV- HNSCC patients with HD TEMRA proportion >34% in peripheral circulation were 18 times more likely to have disease recurrence within six months following surgery. In the peripheral blood, HD TEMRA cells are highly active, with enhanced production of cytolytic enzymes upon stimulation, while patient matched tumor-isolated HD TEMRA produced IFN-γ to a lesser extent. Additionally, we demonstrated that these cells have intact (but impaired) proliferative ability.

Conclusions: To understand the prognostic association of HD TEMRA cells in HNSCC, in-depth characterization of their functional phenotype is required. Here, we demonstrate that HD TEMRA cells display an activated phenotype, with high cytolytic potential. HD TEMRA are found in greater quantity in peripheral circulation than within the tumor environment, and preliminary data indicates tumor infiltrated HD TEMRA produce less cytolytic enzymes than circulating counterparts. Future work will continue to investigate potential differences between HD TEMRA cells based on anatomical location and determine the relationship between HD TEMRA and poor HNSCC prognostication.

Progress and Impact of a Radiology Residency Research Track over a Decade

Presenting Author: Brown, Joshua, MD PhD, Radiology

Poster Number: 4

BROWN, JOSHUA D; Owosela, Babajide; Weinberg, Brent D; Krupinski, Elizabeth A; Mullins, Mark E; Balthazar, Patricia

Background: Radiology is a dynamic and ever-evolving field, necessitating continuous innovation and active research engagement from trainees. However, the conventional training model falls short in fostering research skills, crucial for cultivating the upcoming cohort of physician-scientists. The Emory radiology residency research track (RT) was instituted to offer a specialized research pathway, aimed at developing the next generation of research-focused academic radiologists. The track provides an integrated 4-year longitudinal curriculum and academic time. This study retrospectively assesses the impact and progression of the RT over a decade.

Methods: Using publicly available online data, we collected information on graduates from Emory's radiology residency program between 2014 and 2023 including current position, position type (academic vs. private), and publications. We compared RT and non-research track (NRT) residents.

Results: Out of 147 graduates, 136 profiles (92.5%) were retrievable, including all 14 RT residents. To date, publications per resident was 5.7 (765 total) for NRT residents and 28.6 (401 total) for RT residents. The 2017 cohort produced the most publications per resident with 3.7 (44 total) for NRT residents and 71.5 (143 total) for RT residents. Total citations of publications to date per resident was 69.5 (9673 total) for NRT and 469 (6572 total) for RT. Notably, 37.6% of NRT and 90.0% of RT graduates ($p = 0.005$) are currently affiliated with academic institutions, excluding the 2022 and 2023 graduates who are still completing fellowship training.

Conclusion: Based on our data, residents from the Emory radiology residency research track are more likely to assume academic positions and have a higher number of publications and citations per resident compared to their non-research track counterparts, suggesting it serves as an effective pipeline for cultivating academic radiologists. The insights derived from this evaluation show the potential benefits of incorporating specialized research pathways in radiology residency programs which can enrich the academic radiology landscape.

Utility of MENSA (Media Enriched with Newly Synthesized Antibodies) from Newly-minted Antibody Secreting Cells (ASC) to Diagnose Respiratory Infections

Presenting Author: Capric, Violeta, MD, SOM

Poster Number: 5

Violeta Capric1, Natalie Haddad1, Andrea Morrison-Porter1, Jiwon Park1, Doan C. Nguyen1, Ignacio Sanz2,3, F. Eun-Hyung Lee1,3 1Divisions of Pulmonary, Allergy, Critical Care & Sleep Medicine, 2 Rheumatology, 3Lowance Center for Human Immunology

Background: Diagnosing upper respiratory viral infections (URI) by rapid antigen testing can be problematic due to low viral levels in the airway. This is especially problematic in adults with repeat infections of the same virus. Here, newly-minted antibody-secreting cells (ASC) or plasmablasts in the

blood offer a unique immune snapshot from the antibodies that they secrete to pinpoint the cause of the acute infection. Previously, Elispot assays captured antibodies from these newly-minted ASC and confirmed in 50 patients with RSV (N=40) and influenza virus infections (IAV) (N= 10)1,2. Here, we asked whether this novel matrix called MENSA (Media Enriched with Newly Synthesized Antibodies), a SMART fluidTM could diagnose an unknown URI.

Methods: We enrolled one 70-year-old man 10 days after wheezing, cough, and fever. A nasopharyngeal swab (NPS) was negative for RSV, IAV, and SARS-CoV-2. Six months previously, he was immunized with RSV, IAV, and SARS-CoV-2 vaccines. MENSA and serum were tested on a multi-bead Luminex platform for IgG specific to SARS-CoV-2, Influenza virus, RSV, Tetanus, Epstein Barr Virus (EBV), Cytomegalovirus (CMV), and Herpes Simplex virus2 (HSV2).

Results: As expected, the serum (his historical record) was positive for SARS-CoV-2, IAV, RSV, EBV, and tetanus from previous infections and/or immunizations. The MENSA assays were only positive for RSV and not SARS-CoV-2, IAV, EBV, or tetanus. Elispots confirmed the diagnosis of RSV infection in the peripheral blood mononuclear cells (PBMC). CMV and HSV2 were negative in the serum and MENSA.

Conclusions: Blood MENSA assays offer a unique immune snapshot that can diagnose acute respiratory viral infections with high sensitivity and specificity with a longer time window for diagnosis compared to NPS rapid antigen and PCR testing.

1. Lee FE, Falsey AR, Halliley JL, Sanz I, Walsh EE. Circulating antibody-secreting cells during acute respiratory syncytial virus infection in adults. J Infect Dis 2010;202:1659-66.

2. Lee FE, Halliley JL, Walsh EE, Moscatiello AP, Kmush BL, Falsey AR, Randall TD, Kaminiski DA, Miller RK, Sanz I. Circulating human antibody-secreting cells during vaccinations and respiratory viral infections are characterized by high specificity and lack of bystander effect. J Immunol 2011;186:5514-21.

Antenatal Butyrate Supplementation Improves Intestinal Barrier in Neonatal Murine Offspring

Presenting Author: Colarelli, Andrea, MD, Pediatrics

Poster Number: 6

COLARELLI, ANDREA: and Barbian, Maria Estefania

Necrotizing enterocolitis (NEC) is a disease that primarily affects premature infants and can cause intestinal inflammation and necrosis, with mortality rate of 24%. An important driver in its pathophysiology is impaired intestinal barrier function, which may lead to bacterial translocation and excessive inflammation. Butyrate, a short-chain fatty acid, maintains colonic homeostasis, specifically

intestinal barrier function, by upregulating tight junction (TJ) proteins. Our goal is to determine if antenatal butyrate supplementation (ABS) improves the intestinal barrier in neonatal offspring.

Mating pairs of C57Bl/6 mice received standard water (Control) or 90 mmol of sodium butyrate in their drinking water during pregnancy. In vivo intestinal permeability was analyzed in offspring from each treatment group at post-natal weeks 1, 2, or 3. Offspring were fasted for 4 hours, then gavaged with 20 µl/g of Fluorescein isothiocyanate-labeled 4.4-kDa dextran (FD4). After 4 hours, offspring were euthanized, and blood was collected. Serum FD4 concentration was determined by fluorescence spectroscopy. High serum FD4 suggests leaky intestinal barrier. Samples of ileum and colon were collected for future qRT-PCR analysis of TJ proteins.

2-week-old ABS offspring had lower serum FD4 compared to age-matched controls, though not statistically significant ($p=0.07$). There was a decrease in serum FD4 in control offspring as post-natal age increased ($p=0.03$). While serum FD4 was unchanged in ABS offspring as post-natal age increased, the level was similar to that of 3-week-old control offspring. The change in serum FD4 over time and between ABS and control groups was statistically significant ($p=0.02$ and $p=0.002$, respectively).

Based on this preliminary data, antenatal butyrate supplementation in mice promotes intestinal maturity in neonatal offspring. 1 and 2-week-old offspring exposed to ABS had serum FD4 concentration similar to 3-week-old control offspring. This suggests the intestinal barrier of these mice is more intact. Our sample size in each group was small; thus, we will increase our sample size to better characterize ABS' effect. Next, we will assess expression of TJ proteins in the ileum and colon of these offspring. Finally, we plan to evaluate intestinal barrier function after exposure to a model of neonatal gut inflammation to better represent the pathophysiology of NEC.

A Shock and Kill Cure Strategy for SIV-Infected Infant Macaques: Utilizing a Combination of a Broadly Neutralizing Protein Delivered Through AAV9 and a Latency Reversal Agent

Presenting Author: Fonseca, Jairo, MD, Pediatrics

Poster Number: 7

FONSECA, JAIRO ANDRES; King, Alexis C; Farinre, Omotayo; Liang Shan; Da Costa, Lucas; Enhert, Stephanie; Wood, Jennifer; Gardner Matthew; Van Rompay, Koen; Cottrell, Mackenzie; Martins, Mauricio; CHAHROUDI, ANN.

Background: Latency reversal and clearance represents an HIV cure strategy aimed at reactivating and subsequently eliminating latently infected CD4+ T cells. eCD4-Ig is a fusion protein composed of the ectodomain of CD4, an IgG Fc portion, and the tyrosine-sulfated regions of CCR5 at its carboxy terminus. eCD4-Ig can enhance antibody-mediated cellular cytotoxicity (ADCC), rendering it a promising clearance agent. To improve the recognition of SIV-infected CD4 T-cells by eCD4-IgG, our

strategy incorporated the use of AZD5582, a non-canonical NFκβ stimulator known as a potent latency reversal agent in adult rhesus macaques.

Methods: 72 infant rhesus macaques underwent screening for neutralizing antibodies against AAV9, and twenty were selected, of which 17 exhibited < 25% and 3 showed ≤ 35% AAV9 neutralization. These twenty macaques were orally infected with SIVmac251 at 4 weeks of age and initiated on ART at day 21 post-infection. Simultaneously, half of the macaques received an intramuscular injection of AAV9-eCD4-IgG1. An IgG1 version of eCD4-Ig was chosen for its enhanced antibody effector functions. Previous studies indicated that the latency reversal effect of AZD5582 was less pronounced in infants compared to adults due to drug metabolism differences. Pharmacodynamic modeling was conducted to determine the appropriate infant dose before administering AZD5582 to the infant macaques at 40 weeks post-infection.

Results: All animals exhibited peak SIV RNA levels in plasma of ≥10^7, with ART initiation resulting in at least a 3-log reduction of viral loads within the first two weeks of therapy. eCD4-IgG1 expression exceeding 10 mg/ml was observed in all treated macaques, with sustained protein expression for at least 10 weeks. Pharmacokinetic modeling revealed that higher doses and longer infusion durations are required to replicate the adult pharmacokinetics of AZD5582.

Conclusions: AAV-9 demonstrates promise as a delivery platform for HIV-neutralizing molecules, including bNAbs, due to its long-lasting transgene expression. Higher doses and longer infusion durations are necessary to replicate the adult pharmacokinetics of AZD5582 in infant macaques. Currently, the ability of a higher AZD5582 dose to induce SIV viremia is under evaluation. We hypothesize that this novel cure strategy will lead to the clearance of reactivated latently infected cells via eCD4-IgG1-mediated ADCC.

Unraveling A Role For the Checkpoint Molecule Siglec-15 In Lymphomas

Presenting Author: Francis, Dailia, MD, PhD, Pediatrics

Poster Number: 8

Francis, Dailia B.; Dougan, Jodi; Pillsbury, Claire E.; Park, Sunita; Langermann, Sol; Koff, Jean; Li, Ziyi; Flowers,Christopher and Porter, Christopher

Background: Non-Hodgkin's lymphomas (NHL) are a heterogenous group of hematologic malignancies occurring in children, adolescents, and adults. Intensive multiagent chemotherapy regimens has dramatically improved the 5-year event free survival for these patients. However, for relapsed/refractory (r/r) disease outcomes remain dismal. Despite the integration of hematopoietic stem cell transplant as well as evolving immunotherapies including checkpoint inhibitors survival remains unacceptably low at <30% in the r/r setting highlighting an urgent unmet need for new and effective therapies in this population.

Siglec-15 (Sig-15), an immunoglobulin-like lectin, is a critical immune suppressor that is highly expressed in various human cancers and intra-tumoral myeloid cells. Importantly, inhibiting Sig-15, either through genetic knockout or knockdown, had a restorative effect on local anti-tumor immune responses and abrogated tumor progression. While reported in solid malignancies, a role for Sig-15 in promoting disease progression in lymphomas has not yet been described.

Methods: Sig-15 expression was evaluated in primary human lymphoma patient samples as well as various lymphoma (human and mouse) cell lines using western blot, quantitative PCR as well immunohistochemistry and immunofluorescence methods. Sig-15 expression was inhibited through genetic downregulation in the well-established murine lymphoma cell line A20 and injected into immune competent and immune deficient mice to determine the effect on tumor progression and survival.

Results and Conclusions: Immunohistochemistry of a tumor microarray and validation samples from children shows high Sig-15 expression in NHL samples with distinct staining patterns based on subtype. Specifically, Sig-15 appears to be highly expressed and associated with the cell membrane in most DLBCL and Burkitt's lymphoma, with more variable expression in anaplastic large cell lymphoma, primarily in the cytoplasm at low levels and/or in cells with morphology consistent with macrophages. Stimulation of NF-kB signaling induces increased expression of Sig-15 in lymphoma cells and appears to stabilize Sig-15 in the presence of concurrent inhibition. In addition, preliminary data suggest more than one isoform of Sig-15, raising the possibility of alternative functions. Lastly, knockdown of Sig-15 in A20 cells abrogates disease progression in immune competent but not immunodeficient recipients, consistent with a role for Sig-15 in immune evasion in lymphoma. Together, these data implicate Sig-15 as an immune checkpoint that may be inhibited therapeutically to promote an immune response to lymphoma cells.

Minimizing Chronic Kidney Disease (CKD) Underdiagnosis Using Machine Learning

Presenting Author: Giuste, Felipe, PhD, School of Medicine

Poster Number: 9

Lawrence Huang, Sachin Shankar, Keyvon Rashidi, Dany Alkurdi, FELIPE GIUSTE

Background: Chronic Kidney Disease (CKD) is a prevalent and devastating progressive disease affecting up to 14% (over 35.5 million individuals) of the United States population and costing Medicare well over $64 billion annually. According to the CDC, as many as 90% of individuals with CKD do not know they have it, indicating a significant need for better approaches to detect CKD and prevent unnoticed disease progression.

Methods: This study seeks to address this challenge by developing a data-driven tool to assess patients' CKD risk automatically from available electronic healthcare records. We leveraged a large open-source database of electronic health records (MIMIC-IV dataset) from over 300,000 patients

which has not previously been applied for CKD prediction. Machine Learning (ML) methods were used to develop a software tool to detect the presence of CKD using only patient demographic data, vital signs, and past medical history.

Results: Of the three ML models developed in this study, a random forest classifier had the best performance in predicting CKD presence with an accuracy of 87.5% and an area under the receiver operating characteristic curve (AUROC) of 92.7%.

Conclusions: Our results indicate that ML-based approaches can facilitate screening for patients at risk of progressive diseases like CKD without additional blood tests. We hope our approach may be applied to other under-detected progressive diseases to increase patient awareness and facilitate appropriate long-term management with the goal of improving patient quality of care.

Filling the Tank: A Multi-center Investigation of Trauma Survival After Ultra-massive Transfusion

Presenting Author: Grady, Zachary, MD, Department of Surgery

Poster Number: 10

GRADY, ZACHARY; Meyer, Courtney; Nguyen, Jonathan; Zhang, Ashling; Nekooei, Negar; Filiberto, Dina; Gutierrez, Adam; Risinger, William; McNickle, Allison; Kumar, Athriya; Sanderfer, Van; Sciarretta, Jason; and Smith, Randi

Background: Ultra-massive transfusion (UMT), defined as transfusion of at least 20 units of red blood cell products in the first 24 hours, is rare a procedure that requires significant resource utilization and is associated with high mortality. The aim of this study was to identify patterns associated with survival in patients undergoing UMT.

Methods: A retrospective, multicenter analysis from eight high-volume trauma centers included traumatically injured patients over the age of 12 who received UMT (≥ 20 units RBC/24hr) from 11/2016 - 06/2023. Demographic, clinical, and outcome data were obtained and compared between survivors and non-survivors. The primary outcome was blood product utilization and secondary outcome was types of injury sustained.

Results: A total of 923 patients received UMT with an overall survival rate of 36.8%. Between survivors and non-survivors, there was no difference in mechanism of injury. However, survivors presented tachycardic (116 vs 86, p=0.002), had a higher initial GCS (10 vs 7, p=0.006), higher initial platelet count (189 vs 149, p=0.005), and smaller base deficit (10.6 vs 15.3, p=0.03). Non-survivors presented with a lower initial SBP (81.6 vs 99.5, p=0.0004) and higher initial lactate (10.9 vs 7.9, p=0.001). Survivors underwent fewer ED thoracotomies (5.3 vs 34.3%, p=0.01), fewer exploratory laparotomies (70.9 vs 83.9%, p<0.001), but more extremity explorations (24.7 vs 14.9%, p=0.001). There were more solid organ injuries in non-survivors (49.6 vs 41.2%, p=0.014) however survivors had more extremity vascular injuries (22.4 vs 13.7%, p=0.001). Survivors more frequently underwent emergent IR

procedures (28.8 vs 23.0%, p=0.049) and required less RBC (5.9 v 8.0L, p=0.006), less FFP (3.8 vs 5.2L, p=0.008), and less platelets (699 vs 860mL, p=0.005).

Conclusion: Patients who require UMT have signficant rates of mortality. However, better compensated shock, a higher initial GCS, the absence of an ED thoracotomy, and presence of an extremity vascular injury may be associated with improved rates of survival.

Cobalamin Deficiency in Children with Sickle Cell Disease

Presenting Author: Hatabah, Dunia, MD, Emory University

Poster Number: 11

Hatabah, Dunia; Krieger, Rachel; Brown, Lou Ann; Harris, Frank; Korman, Rawan; Benedit, Laura; Umana, Jasmine T; Rees, Chris A; Dampier Carlton; Morris, Claudia R

Background: B12-deficiency has been reported in 18% of adults with SCD vs 10% without SCD. There is limited and contradictory data on the prevalence of B12-deficiency in children with SCD. Diagnosis of B12-deficiency is challenging, with no gold standard; no data exists to guide B12-deficiency screening in patients with SCD. Adding to the urgency of addressing B12-deficiency risk in SCD is the increased use of nitrous oxide gas (N2O) in the United States. Pertinently, N2O is standard therapy for SCD-pain in Europe. N2Oimpacts B12 metabolism, with reports of neurologic sequalae in patients with SCD treated with N2O emerging.

Objective: To evaluate prevalence of B12-deficiency in children with SCD-pain in a pediatric emergency department (ED).

Methods: This is a secondary analysis of samples collected as part of ED-based clinical trials enrolling children with SCD-pain, evaluating mechanisms of hemolysis. B12-deficiency was defined as plasma MMA >318 nmol/L or urine MMA/Cr ≥2.2 mmol/mol.

Results: A total of 94 children (13±4 years, 54% female, 68% hemoglobin SS disease, and 72% on Hydroxyurea) were included. Fifty-two percent (49/94) had B12-deficiency diagnosed by either urine MMA/Cr, plasma MMA or both. Twenty-six percent (24/94) of patients were B12-deficient based on urine MMA/Cr, while 39% (37/94) were diagnosed by elevated plasma MMA. Of all subjects found to be B12-deficient by either plasma or urine, 12 children (13%) were diagnosed with B12-deficiency identified in both plasma and urine. There were no significant differences in patient demographics or clinical characteristics in B12-deficient vs non-deficient groups. Plasma MMA and urine MMA/Cr showed no correlation with hemoglobin and MCV.

Conclusion: Our data confirms that B12-deficiency is common in children with SCD, with a concerning prevalence of 52%. Given challenges with reliability of testing modalities, it is not possible to determine whether this is an over- or under-estimation of the true prevalence. Nonetheless, given the safety, affordability, and effectiveness of B12 supplementation, alongside current practices of

administering folic acid to patients with SCD despite scarcity of evidence, it seems prudent to also consider incorporating B12 supplementation into our management regimen, to avoid detrimental consequences of an easily treatable cobalamin deficiency.

Association of Age with Acuity and Severity of Illness at Initial Presentation and Mortality in Children, Adolescents, and Young Adults with Leukemia

Presenting Author: Jain, Tarun, MD, Pediatrics

Poster Number: 12

Jain, Tarun; Ji, Xu; DeGroote, Nicholas; Himes, Alexandra; Coxhead, Cortland; Khanna-Farber, Anjali; Cathcart, Alexandra; Miller, Tamara P.; Blum, Kristie A.; Tarquinio, Keiko M; and Castellino, Sharon M.

Background: Patients ≥ 10 years of age with leukemia are at higher risk for mortality than younger patients. Acuity and severity of illness in older versus younger patients have been understudied.

Objective: Determine age's association with acuity or severity of illness and mortality in patients presenting with new leukemia.

Design/Method: We performed a retrospective analysis of 688 patients aged 1-21 years who presented with leukemia at Children's Healthcare of Atlanta between 2010-2018. High acuity of illness was defined as any intensive care unit resource use in the first 72 hours following presentation (yes/no). High severity of illness was defined as initial white blood cell count ≥ 50,000 cells/microliter or central nervous system disease (yes/no). Multivariable logistic regression was used to determine age's association with high acuity or severity of illness, controlling for sex, race/ethnicity, insurance, and leukemia type. Survival and mediation analysis were performed using Kaplan-Meier curves and Cox proportional hazard regression.

Results: The median age of the cohort was 6 years (interquartile range 3-12 years, 65.7% aged 1-9 years, 34.3% aged 10-21 years), 53.8% were male, 48.1% were non-Hispanic White, and 41.9% had private insurance. Diagnoses included B-cell acute lymphoblastic leukemia (ALL) (68.3%), AML (16.7%), T-cell ALL (10.8%), and other leukemias (4.2%).

High acuity of illness was more likely in older patients [OR 10-21 vs. 1-9 years: 1.94 (1.32-2.85)]. Age group was not significantly associated with high severity of illness [OR 10-21 vs. 1-9 years: 1.25 (0.88-1.78)]. High acuity, but not high severity, was associated with higher risk of death [HR high vs. low acuity at 1-year: 2.10 (1.14-3.92)] and while not significant, explained 15% (-4 – 35%) of mortality differences by age group.

Conclusion: Older patients were more likely than younger patients to have high acuity of illness, which was associated with elevated mortality, indicating disparities from the point of initial presentation. This research will help inform strategies toward narrowing age disparities in leukemia outcomes.

Exploring Novel Mechanisms of Platelet Clearance to Mitigate Thrombocytopenia in Patients Refractory to Transfusion.

Presenting Author: Jhita, Navdeep, MD, Pathology

Poster Number: 13

JHITA, NAVDEEP; Kyu, Shuya Y; Albizua, Igor and Maier, Cheryl L.

Background: Platelet transfusion is an essential therapy for prevention and treatment of bleeding, with millions of units transfused each year. However, up to 44% of platelet transfusions fail to achieve the anticipated platelet count, leading to increased patient morbidity and mortality. This is described as platelet refractoriness (PR), which may be of immune or nonimmune etiology. Administration of treatments, like intravenous immunoglobulin, that are efficacious for other causes of thrombocytopenia have yielded variable results in PR, pointing to differences in the mechanisms underlying platelet clearance. Thus, greater understanding is needed to elucidate the pathways involved in platelet clearance in patients with PR. Recently, CD8 T cells have been found to play a role in the accelerated clearance of transfused allogeneic platelets. Data demonstrate that CD8 T cells do not induce allogenic platelet clearance through canonical mechanisms of cellular toxicity. Rather, CD8 T cell interaction induces platelet activation, which may cause activation-induced desialylation and result in clearance through the hepatic asialoglycoprotein receptor. Here we aimed to explore the disialylation events on platelets after allogeneic CD8 T cell interation and investigate the ability of a sialidase inhibitor, Oseltamivir Phosphate (OP), to improve donor platelet survival after transfusion.

Methods: A murine model of platelet refractoriness using transgenic strains (OTI and mOVA) was used. OTI or wild type (WT) control recipient mice were loaded with three doses of OP or vehicle control every 8 hours and transfused CFSE-labeled platelet rich plasma (PRP) from mOVA or WT donors via lateral tail vein. The rate of platelet clearance was assessed by measuring platelet survival sampling at 1hr and 24hr by flow cytometry.

Results: The rate of clearance of transfused mOVA platelets in OTI recipients was 40% faster than its corresponding WT control group. OTI recipients receiving OP displayed similar clearance rates as those not receiving OP.

Conclusions: Preliminary data do not demonstrate any beneficial role of OP in improving donor platelet survival in our murine model of PR. Further exploration of the mechanism of desialylation and its effects on transfused platelet clearance are underway. Future experiments will include different routes of OP administration, as hepatic activation of OP is anticipated to be important.

Kyotorphin: A Novel Mechanism-of-action for Arginine Therapy Targeting Vasoocclusive Pain Episodes (VOE) in Children with Sickle Cell Disease (SCD)

Presenting Author: Korman, Rawan, MD, Emory University School of Medicine Department of Pediatrics

Poster Number: 14

Korman, Rawan; Hatabah, Dunia; Brown, Lou Ann; Harris, Frank; Bakshi, Nitya; Archer, David R; Rees, Chris A; Griffiths, Mark A; Benedit, Laura; Dampier, Carlton; MORRIS, CLAUDIA R

Background: Low arginine bioavailability is associated with SCD mortality and morbidity, including acute pain severity. Multiple phase 2 trials support the safety & efficacy of arginine therapy in children with SCD-VOE. As the obligate substrate for nitric oxide(NO) production, arginine's mechanism-of-action is unknown but thought to be related in part to NO, a potent vasodilator. Kyotorphin is an endogenous opioid-like analgesic composed of the amino acids tyrosine and arginine. Oral arginine given to wild-type mice increases kyotorphin levels centrally. The association between arginine supplementation as a precursor to kyotorphin in SCD is unknown.

Objective: Determine the impact of intravenous(IV) arginine on plasma arginine, kyotorphin, and NO metabolite (NOx) concentrations and their association with pain scores in children hospitalized with SCD-VOE.

Methods: A pharmacokinetics/pharmacodynamics study of hospitalized children aged 7-21 years with SCD-VOE randomized to receive one of 3 dosing arms of IV arginine: 1)100mg/kg TID(n=4); 2) 200mg/kg once followed by 100mg/kg(n=5); or 3) 200mg/kg followed by continuous infusion (300mg/kg/day) until discharge(n=4). Plasma arginine, kyotorphin, and NOx were measured through previously described methods. Daily numeric pain scores (0-10) were collected. Mean±SD, paired t-tests, and Pearson correlation analyses between groups were performed where appropriate.

Results: 13 patients (13±3 years, 62% males, 85% HbSS, 92% on Hydroxyurea) were enrolled. Plasma arginine and kyotorphin concentrations significantly increased and peaked at 1 hour after infusion initiation ($p<0.001$, $p=0.004$ respectively) with no significant differences in peak concentrations between study arms. Kyotorphin levels strongly correlated to plasma arginine concentration ($r=0.72$, $p<0.0001$). Plasma NOx levels also significantly increased after IV arginine infusion from pre-dose, with a mean absolute maximum change of 12.1±16.2μM ($p=0.02$). Day 2 pain scores significantly and inversely correlated with peak kyotorphin levels on Day1 of the pharmacokinetics study and with change in plasma arginine concentration(mM) from baseline to discharge in subjects receiving an arginine loading dose.

Conclusion: IV arginine therapy increased plasma arginine concentration 2-5 times above baseline, peaking within 1 hour of infusion initiation. We report for the first time the that IV arginine increases kyotorphin in SCD. This may represent a novel opioid-sparing mechanism-of-action for arginine with implications for pain syndromes beyond SCD.

Combination cIAP and BCL-2 Inhibition to Induce Latency Reversal and Apoptosis in SIV-infected, ART-suppressed Rhesus Macaques

Presenting Author: Lampros, Elizabeth, Bachelor of Science, Department of Pediatrics

Poster Number: 15

Lampros, Elizabeth; Ukhueduan, Benedicth; Sonawane, Soham; Endrias, Kedan; Siddiqi, Zain; Lopez, Lakshita Lopez; Schoof, Nils; Mavigner, Maud; Schauer, Amanda; Cottrell, Tompkins, Lauren; Mackenzie Leigh; Lifson, Jeffrey; Keele, Brandon; Chahroudi, Ann

Background: While antiretroviral therapy (ART) effectively controls HIV replication, the persistent reservoir of latently infected CD4+ T cells poses a formidable challenge to achieving a cure. In this nonhuman primate study, we hypothesized that a synergistic approach combining the cIAP-inhibitor AZD5582 (AZD) with the BCL-2 inhibitor Venetoclax (VTX) could reverse latency and augment the clearance of reactivated infected cells through apoptosis.

Methods: Thirty intravenously SIVmac239M-infected rhesus macaques (RMs) were initiated on ART at 4 weeks post-infection. At 68 weeks post-infection, RMs were divided into three treatment groups: A) ART only, B) ART + VTX, C) ART + VTX + AZD. VTX was dosed at either 15 mg/kg intramuscular or 300 mg oral, with 3 cycles of 4 daily doses in groups B and C. Additionally, Group C received 10 weekly intravenous infusions of AZD5582 at 0.1 mg/kg. Analytical treatment interruption (ATI) commenced after 14 weeks of intervention. Weekly plasma viral loads were obtained during intervention and ATI. Whole blood was stained, and absolute T and B cell counts were assessed by flow cytometry.

Results: AZD induced latency reversal, measured by on-ART viremia in 6 of 10 RMs in Group C, with peak levels reaching 1100 copies/ml. VTX induced a transient decrease in CD4+, CD8+, and CD20+ lymphocytes, with reconstitution evident prior to the end of the intervention. Following ATI, no significant differences in time to rebound or peak viral load were observed across the three arms. Follow up post-rebound is still ongoing, with some animals in each group demonstrating post-ART viral control after 3 months (A: 5/10, B: 7/10, C: 4/9).

Conclusions: While the combination of AZD5582 and Venetoclax did not result in delayed viral rebound after ART interruption, treatment effects were discernible through on-ART viremia induction and temporary lymphocyte reductions. Our study provides important insight into the significant challenge of eliminating rebound-competent reservoirs following established SIV/HIV infection.

Convenience versus Correlation: Lack of Agreement amongst Point-of-Care Platelet Function Testing Platforms and Light Transmission Aggregometry

Presenting Author: Laskey, Emily, MD/PhD Program (M3), School of Medicine

Poster Number: 16

Laskey,Emily; Achram, Robert; Barrette, Eileen; Guarner, Jeannette; Smith, Geoffrey; and Maier, Cheryl

Platelet function testing (PFT) is critical for determining the efficacy of dual antiplatelet therapy (DAPT) to prevent thromboembolic complications in patients undergoing surgical intervention. Light

transmission aggregometry (LTA) is an absorbance-based assay that has historically been the gold standard for assessing platelet function. However, as LTA is a laboratory-based method that requires the use of skilled laboratory technicians and prepared plasma samples, clinicians are opting for the implementation of more convenient point-of-care (POC) testing methods in the operating room and clinic. Compared to LTA, POC testing methods such as thromboelastography (TEG) mapping and VerifyNow offer the advantage of providing rapid results without the need for skilled laboratory personnel. Despite the popularity of TEG and VerifyNow, these methods have yet to be compared to the gold standard of PFT (LTA). This study aims to assess the agreement between LTA, VerifyNow, and TEG platelet mapping to determine if these whole blood, POC testing methods are an adequate, at-the-bedside replacement for LTA. A total of 24 blood samples were analyzed and the maximum percent of platelet aggregation (a measurement of platelet function) was recorded in response to either an adenosine diphosphate (ADP) agonist (to assess PY12-inhibitor response) or an arachidonic acid (AA) agonist (to assess aspirin response). Samples were then characterized as either optimally or suboptimally suppressed for each platform based on established values. The agreement was calculated using the following formula (optimal/optimal + suboptimal/suboptimal) / total number of samples and the Pearson correlation coefficient between the values for each platform was calculated using a linear fit. Overall agreement between the platforms ranged from 47 – 69% with no significant correlation in measurements of platelet function. The variability in the platforms indicates the need for further investigation before whole blood, POC testing methods can be used as a replacement for LTA in assessing adequate platelet suppression in patients receiving DAPT.

Imaging poly(ADP-ribose) polymerase-1 with a novel 18F-labeled brain penetrant PET ligand

Presenting Author: Patel, Jimmy, MD, PhD, Radiation Oncology

Poster Number: 17

Patel, Jimmy S.; Zhou, Xin; Chen, Jiahui; Li, Yinlong; Rong, Jian; Gao, Yabiao; Zhao, Chunyu; Chaudhary, Ahmad F.; Schuster, David M.; and Liang, Steven H.

Background: Poly(ADP-ribose) polymerase (PARP) inhibitors are increasing in clinical utility. The ability to detect PARP1 expression and distribution in patients would provide clinicians with valuable information of treatment design and monitoring response. Current PARP PET ligands face limitations in their capacity to penetrate through the blood-brain-barrier (BBB), thereby impeding their efficacy in detecting PARP1 in the brain. Herein we present the development of 18F-AZD9574, a novel PET ligand distinguished by its PARP1 selectivity and brain permeability.

Methods: AZD9574 underwent radiolabeling with fluorine-18 via nucleophilic displacement. A comprehensive analysis, including molecular docking, IC50 measurement, microsomal & plasma stability and cellular uptake using PC-3 cells, was conducted. Autoradiography was performed on rodent/nonhuman primate (NHP) brain tissues and PET imaging studies were conducted in NHPs.

Results: AZD9574 and its 18F analog were synthesized, with molecular docking revealing key interactions in PARP1 homolog models. AZD9574 exhibited high PARP1 potency and selectivity with an IC50 of 1.2nM and >1μM against PARP1 and PARP2, respectively. In addition, 18F-AZD9574 was found to show excellent stability in liver microsome (rat/human) and plasma (rat/NHP/human) within 90 minutes. 18F-AZD9574 demonstrated high in vitro specific binding in PC-3 cell lines in a dose response manner. While blocking with AZD9574 and Olaparib led to decreased uptake, no blockade was observed when using UPF-1035, a PARP2 specific inhibitor, supporting high binding selectivity of 18F-AZD9574 towards PARP1. Autoradiography indicated heterogeneous brain uptake (cerebellum, hippocampus>pons in rodents and high uptake in cerebellum in NHPs), with decreased brain uptake in the presence of PARP inhibitors. PET imaging of NHP showed highest uptake in the cerebellum, followed by hippocampus, and the lowest in the pons and white matter. Blocking with AZD9574 demonstrated dose dependent specific binding.

Conclusion: We have successfully validated 18F-AZD9574 as a potent and selective PARP1 PET ligand. The preclinical data presented in this work suggests that 18F-AZD9574 may serve as a novel molecular imaging tool for selective and specific imaging of PARP1 in vivo. This holds great promise for identifying PARP1-related pathologies within the human brain.

Clinical predictors of Spontaneous Intestinal Perforation vs Necrotizing Enterocolitis in extremely and very low birth weight neonates

Presenting Author: Dantes, Goeto, MD, Surgery

Poster Number: 18

Olivia A. Keane, MD, Louis Do, BS, Savanah Rumbika BS, Nathaniel H. Ellis, BS, Valerie L. Dutreuil, MPH, Zhulin He, PhD, Amina M. Bhatia, MS, MD

Purpose: Spontaneous intestinal perforation (SIP) and necrotizing enterocolitis (NEC) are distinct disease processes associated with significant morbidity and mortality, particularly in extremely low (ELBW) and very low birth weight (VLBW) neonates. Early and accurate diagnosis is important as appropriate treatment, laparotomy (LP) versus initial trial of peritoneal drainage (PD), is key to improving outcomes. However, both clinical presentations often overlap and can be difficult to distinguish preoperatively. Our study investigated clinical characteristics associated with each diagnosis and constructed a scoring algorithm for accurate preoperative diagnosis.

Methods: A cohort of ELBW (<1000g) and VLBW (<1500g) neonates surgically treated for suspected SIP or NEC between 07/2004-09/2022 (n=367) at two level IV NICUs were reviewed. Patients with incomplete charts, transfers or death immediately following drainage, or patients treated for NEC medically prior to diagnosis, were excluded. Clinical characteristics evaluated included gestational age (GA), birth weight, feeding history, preoperative physical exam, and laboratory/radiological findings. Intraoperative diagnosis was used to determine SIP vs NEC. Pre-drain diagnosis was used for patients treated with PD only.

Results: 338 neonates were managed for SIP (n=269, 79.6%) vs NEC (n=69, 20.4%). PD was definitive treatment in 161 (47.6%) patients. Seventy-five (22.2%) patients were treated with upfront LP. There were no significant differences in birth weight, gender, or race/ethnicity. Clinical characteristics associated with SIP compared to NEC included younger GA, younger age at initial intervention (AFI), and history of trophic or no feeds. Abdominal wall erythema, Pneumatosis on X-ray, goal or advancing feeds, and higher C-reactive protein test were associated with NEC. Multivariate logistic regression determined pneumatosis, abdominal wall erythema, higher AFI and history of feeds to be highly predictive of NEC. A 0-8-point scale based on these risk factors was designed with the area under the receiver operating characteristic curve of 0.819 (95% CI 0.756-0.882) for the diagnosis of NEC. A threshold score of 1.5 had a specificity of 0.952and sensitivity of 0.652.

Conclusion: Utilizing important clinical characteristics associated with SIP & NEC we developed a point of care scoring system designed to assist surgeons accurately distinguish SIP vs NEC in VLBW/ELBW neonates.

Uremic Milieu Induces Cellular Reprogramming in Aortic Cells in a Mouse Model of Chronic Kidney Disease

Presenting Author: Reyes, Loretta, MD, Pediatrics

Poster Number: 20

REYES, LORETTA; Park, Christian; Villa-Roel, Nico; Li, Haiyan; Kang, Dong-Won; and Jo, Hanjoong

Introduction: Chronic Kidney Disease (CKD) is a progressive condition marked by high cardiovascular morbidity and mortality. CKD has profound effects on vascular health, including the characteristic arterial uremic vasculopathy, which manifests as arterial wall calcification and pathologic vascular remodeling with resultant increased arterial stiffness and end-organ damage. The aorta contains numerous cell types that can contribute to vascular remodeling therefore we hypothesized that the uremic milieu of CKD reprograms arterial cells leading to the uremic vasculopathy phenotype, and conducted single-cell RNA sequencing (scRNAseq) to define the transcriptomic landscape in the mouse aorta.

Methods: CKD was induced via 5/6 nephrectomy in 2 cohorts of SvJ/129X mice; non-surgical controls were included for comparison. Single cell suspensions prepared from collagenase digestion of the descending thoracic aorta at 4 weeks (cohort 1; CKD n=4, control n=4) and 8 weeks (cohort 2; CKD n=4, control n=4) were used for scRNAseq analysis. Cell clusters and differentially expressed genes were determined using Seurat R-package.

Results: Unsupervised cluster analysis from 21,721 aortic cells identified 20 distinct cell clusters representing 8 cell types (endothelial cells (ECs), smooth muscle cells (SMCs), fibroblasts (FBs), macrophages (MΦs), and other immune cells (T-cells, B-cells, neutrophils, mast cells). ECs, SMCs and FBs were the predominant cell types in the control group, however there was a relative decrease in

the SMC population in CKD with a concomitant increase in the immune cell population, especially MΦs, T-cells and neutrophils. CKD resulted in EC sub-populations with overexpression of pro-inflammatory/proliferative genes, as well as endothelial-to-mesenchymal transition (EndMT) and endothelial-to-immune transition (EndIT) genes compared to controls. CKD also induced a transition from healthy, contractile phenotype to a pro-inflammatory, synthetic phenotype in SMC sub-populations. Interestingly, we identified a FB sub-population, only present under CKD conditions, that over-expressed complement/chemokine genes (C3, C4b, Cfb, Cxcl12).

Conclusion: Overall, our results demonstrated an increased proportion of immune cells in the aorta in CKD and we identified a transition to a pro-inflammatory, proliferative phenotype in several cell lines and cellular over-expression of genes involved in immune system activation. Together, our data suggests inflammation plays a key role in the development of uremic arterial vasculopathy.

Environmental Justice Index and Healthcare Utilization in Pediatric Patients with Asthma

Presenting Author: Rowland, Annabelle, MD, Pediatrics

Poster Number: 21

ROWLAND, ANNABELLE; Jaggi, Preeti; Lee, Gerald; Hemani, Sunita; Lovelace, Kyle; and Orenstein, Evan.

Background: A large body of evidence demonstrates the impact environment has on the development of childhood asthma and its outcomes. It is well described that inequities in asthma outcomes exist based on race, socioeconomic status, and urban living. There is growing research describing environmental inequities impacting asthma outcomes. More research is needed regarding the cumulative impact of both social and environmental factors on childhood asthma. The Environmental Justice Index (EJI) is a validated tool from CDC that ranks each U.S. Census tract based on environmental, social, and health factors. The EJI has yet to be applied to a pediatric population. This study aimed to evaluate whether the EJI and its subcomponents are associated with increased risk for asthma exacerbation. We hypothesize that neighborhood-level social and environmental factors are associated with increased risk for asthma exacerbation in urban pediatric populations.

Methods: Our data query identified 65,272 index visits with primary diagnosis of asthma. The index setting included pulmonology, allergy, and primary care clinics within Children's Healthcare of Atlanta. Addresses were geocoded to obtain census tract. 3,435 visits were excluded due to inability to geocode address. The remaining 61,837 represented 1,414 census tracts. Asthma exacerbation was defined as hospitalization or ED visit with primary diagnosis of asthma or oral steroid course. We used multiple logistic regressions to evaluate if social environmental ranking (SER), environmental burden, or social vulnerability was predictive of asthma exacerbation within a 90-day period from index visit. All models were adjusted for sex, race, body mass index, and asthma severity. Sub-groups included season and time periods (2019-2021 vs 2022-2023), which were based off Atlanta city schools resuming in-person classes following COVID-19 pandemic.

Results: Social vulnerability was significantly associated with odds of asthma exacerbation for three seasons (Spring, Summer, Fall) for 2019-2021 time period ($p<0.001$). The SER and environmental burden were not significantly associated with odds of asthma exacerbation.

Conclusions: The EJI demonstrated the impact of neighborhood-level social vulnerability on odds of exacerbation specifically non-winter seasons but did not elucidate neighborhood-level environmental impact on risk of exacerbation for pediatric patients with asthma. Considerations for socioeconomic factors that contribute to asthma exacerbation should be explored.

LIN28B Mediates Resistance to Cisplatin in Group 3 Medulloblastoma

Presenting Author: Shahab, Shubin, MD, PhD, Pediatrics

Poster Number: 22

Shahab, Shubin; Kania, Catherine ; MacDonald, Tobey and Kenney, Anna.

Background: Children with Group 3 medulloblastoma (MB) have a very poor prognosis due to frequent relapsed and refractory disease and a tendency to develop early distant metastasis suggesting their intrinsic therapy resistance. We have recently demonstrated that the LIN28B pathway plays an important role in Group 3 MB growth and proliferation.

Methods: To investigate whether LIN28B mediates therapy resistance in Group 3 MB we treated D341 and HDMB03 Group 3 MB cell lines with low dose cisplatin (below IC50) over several weeks and induced resistance. We then measured LIN28B levels and also did knockdown studies to investigate whether decreased LIN28B increases Group 3 MB sensitivity to cisplatin.

Results: We found that repeated low dose cisplatin treatment increased LIN28B levels in D341 and HDMB03 cells and increased cisplatin resistance (as indicated by increased IC50). We also found that by decreasing LIN28B levels Group 3 MB cells became more sensitive to cisplatin.

Conclusion: Our results suggest that LIN28B is involved in mediating cisplatin resistance in Group 3 MB cells. For future studies we plan to perform correlative studies from patient samples and investigate the exact mechanism of this resistance.

CD26 a Biomarker that can Enhance Response to T Cell Therapy in Advanced Melanoma

Presenting Author: Swisher, Shannon, MD, BS, Department of Surgery

Poster Number: 23

SWISHER, SHANNON; Wyatt, Megan; Cole, Anna; Wittling, Megen; Ruffin, Ayana; Bailey, Stefanie; Nelson, Michelle; Delman, Keith; Lesinski, Gregory; Lowe, Michael; and Paulos, ChrystalSWISHER, SHANNON; Wyatt, Megan; Cole, Anna; Wittling, Megen; Ruffin, Ayana

Background: We identified a novel subset of CD4+ T cells with high levels of CD26 expression that have enhanced stemness and polyfunctionality in vivo. The presence of CD4+ CD26high T cells can predict response to immune checkpoint inhibitor therapy with Nivolumab, and improved progression-free (PFS) and overall survival (OS). Based on this data, we posit that presence of CD26 on T cells can be leveraged to improve cellular therapies in advanced melanoma.

Methods: Mouse models expressing a transgenic TCR specific for tyrosinase on melanoma were used for in vivo studies. Mouse TRP-1 CD4+ T cells were sorted by flow cytometry based on CD26 expression: CD26neg or CD26high T cells and then infused into B16F10 melanoma-bearing mice. Inhibition of CD26 enzymatic activity with sitagliptin [2mM] explored the necessity of enzymatic function to achieve this robust antitumor response. Peripheral blood from healthy donors was compared to pts with metastatic melanoma to quantify, phenotype, and characterize the functionality of CD4+CD26high T cells.

Results: Using a TCR-transgenic system where T cells recognized TRP-1 melanoma Ag, we found that CD4+ CD26high T cells elicit potent antitumor activity in vivo compared to mice infused with CD4+ CD26neg T cells ($P < 0.05$) or no treatment ($P < 0.001$). CD26 enzymatic activity is required for improved tumor regression as sitagliptin impaired TRP-1 CD4+ CD26high T cell function in B16F10 mice with melanoma. At 125 days, 80% of mice that had active CD26 enzyme were alive compared to 10% in the CD26-inhibited group that received sitagliptin, a known CD26 inhibitor. Patients with advanced melanoma have fewer CD4+ CD26high T cells than healthy donors ($P = 0.001$) at baseline and have worse clinical outcomes including decreased PFS ($P = 0.014$) and OS ($P = 0.010$).

Conclusions: We discovered that T cells with high CD26 expression effectively regress solid tumors in vivo, and CD26 enzymatic activity is required for this effect. CD26 expression can improve prognostication in patients advanced melanoma by guiding individualization of treatment regimens. Ongoing analyses aim to reveal the mechanism by which these cells enhance the immune response.

Using Controlled Human Infection with H3N2 Virus to Characterize Shedding Kinetics, Identify Symptomatological Associations, and Develop a Human Influenza Transmission Model

Presenting Author: Tanios, Ralph, MD, MS, Infectious Diseases

Poster Number: 24

Tanios, Ralph; Traenkner, Jessica; Macenczak, Hollie; Smith, Veronica; Buster, Vanessa; Johnson, Brandi; Shephard, Meredith; Shetty, Nishit; Rockey, Nicole; Le Sage, Valerie; Vargas-Maldonado, Nahara; Danzy Bedoya, Shamika; Kraft, Colleen; Marr, Linsey; L

Background: Influenza causes significant disease burden globally. In the United States alone, the Centers for Disease Control and Prevention estimate that sixteen million medical visits, three hundred and ninety thousand hospitalizations, and twenty-five thousand deaths were attributed to Influenza infections during the 2019-2020 season. Although basic science and clinical research broadened our understanding of viral immunology and pathogenesis, important questions regarding correlates of

protection, viral evolution, and transmission remain unanswered. Developing a robust challenge model is essential in understanding the relationship between viral shedding and development of symptoms consistent with mild-to-moderate Influenza disease.

Methods: In this pilot study, we conducted a controlled human Influenza infection model at Emory University's inpatient research unit during the summer of 2022. Eight healthy participants having hemagglutination inhibition titers less than or equal to 1:40 were challenged with seasonal H3N2 influenza virus (A/Perth/16/2009). To study viral shedding kinetics, we collected nasopharyngeal swabs, nasal lavage, and saliva samples up to seven days post-inoculation. To assess for adverse events and investigate associations between viral titers and symptom severity, we queried participants' symptoms using the Evidera InFLUenza Patient-Reported Outcome questionnaire (FLU-PRO).

Results: Six of eight challenged participants tested positive for Influenza by PCR testing and shed virus in nasal cavity and saliva. Four of six seropositive participants exhibited sustained shedding, while two of six exhibited transient shedding. Average onset of seroconversion was 1.5 ± 0.3 days post-inoculation. Average change in hemagglutination inhibition titers was sixty eight in the seropositive group and thirty in the seronegative group. Seropositive individuals tested positive for an average of 4.8 ± 0.9 days of the seven hospital days. The most commonly reported symptoms in seropositive individuals were runny nose and headache. Number of symptoms and symptom severity did not consistently reflect higher viral titers.

Conclusions: Influenza A is shed after controlled human challenge with an attack rate of 75%. The amount of virus shed varies per individual and might not be associated with the number and the severity of symptoms developed. Despite our Influenza challenge model's success, further sample size expansion and inclusion of data on transmission are warranted.

Intravascular Lithotripsy Broadens the Indication for Transfemoral Aortic Valve Replacement

Presenting Author: Tom, Stephanie, MD, Department of Surgery

Poster Number: 25

TOM, STEPHANIE, Tully, Andy, Kikuchi, Yuta, Crawford, Kaylyn, Binongo, Jose, Wei, Jane, Gleason, Patrick, Xie, Joe, Devireddy, Chandran, and Grubb, Kendra

Background: Transfemoral transcatheter aortic valve replacement (TF-TAVR) approach has proven to be superior to alternative access. However, a subset of patients being evaluated for TF-TAVR are deemed unfit secondary to peripheral arterial disease. For patients anatomically unfit for standard transfemoral access, peripheral intravascular lithotripsy (IVL) has emerged to facilitate femoral access for TAVR.

Methods: Single center, retrospective analysis queried from 1/2018 through 7/2023 for all patients undergoing TAVR. All patients undergoing IVL facilitated lithotripsy for transfemoral access were analyzed.

Results: A total 2,862 TAVR cases were identified, with 92 (3.2%) having undergone lithotripsy. The lithotripsy cohort consisted of 45% female with mean age of 78±9.2 years. 59 of the 92 patients underwent multiple treatment segments (64%) with a total of 145 lesions treated. The right common iliac artery (n=47) was most treated. Most lesions fell below 5.5mm (70.3%). Average percent diameter vessel stenosis was 41.1±15.2%. Average maximum arc calcification 171.9±75.2 degrees. Majority of IVL was performed with 7-mm lithotripsy catheter (72.5%). Valve delivery was successful in all cases. The average length of stay was 2.5±2.9 days. Complications requiring secondary vascular procedure occurred in 4.3% (n=4/92). Mortality at 30-days 1.1% (n=1/92).

Conclusions: In 92 consecutive patients, the addition of IVL treatment allowed passage of the TAVR delivery catheter in all cases despite presence of severe calcific disease of the iliofemoral axis. The IVL facilitated TF-TAVR is feasible, safe, and effective at preserving the transfemoral TAVR route in patients with severe peripheral artery disease.

The Prevalence and Topography of Spinal Cord Demyelination and Inflammatory Activity in Multiple Sclerosis

Presenting Author: Waldman, Alex, DPhil, Emory MSTP

Poster Number: 26

WALDMAN, ALEX DAVID; Catania, Cecilia; Pisa, Marco; Jenkinson, Mark; Lenardo, Michael; De Luca, Gabriele

Background: Spinal cord pathology is a major determinant of irreversible disability in progressive multiple sclerosis. The demyelinated lesion is a cardinal feature. The well-characterized anatomy of the spinal cord and new analytic approaches allow the systematic study of lesion topography and its extent of inflammatory activity unveiling new insights into disease pathogenesis. Given the lack of consensus regarding the vascular and cerebrospinal fluid (CSF) contributions to spinal cord pathology, we aimed to characterize the prevalence and topography of spinal cord demyelination in a large post-mortem cohort using immunohistochemistry (IHC), the gold standard method for lesion detection.

Methods: Cervical, thoracic, and lumbar spinal cord tissue derived from 119 MS cases was available for study. IHC was used to detect demyelination (proteolipid protein) and classify its inflammatory activity (CD68). Lesions were standardized onto anatomical templates before mixed models and permutation-based voxelwise analysis were used to identify patterns in the prevalence and topography of demyelination.

Results: Spinal cord lesions were observed in 76.5% of cases with the cervical level being preferentially affected. Lesions were inflammatory in 87.9% of cases. Topographically, lesions consistently affected the dorsal and lateral columns with relative sparing of subpial areas in a distribution mirroring the vascular network. The presence of spinal cord lesions related strongly with clinical disease milestones, including time from onset to wheelchair and onset to death.

Conclusions: Our findings demonstrate that demyelination is common and highly inflammatory, biased towards the cervical level, and relates to clinical disability measures even at late disease stages. The topography of lesions and relative sparing of subpial areas point to a primary role of the vasculature in lesion pathogenesis, suggesting short-range cell infiltration from the blood and signaling molecules in the perivascular space are involved lesion development. These findings challenge the notion that end-stage progressive multiple sclerosis is 'burnt out' and that diffusible factors from the cerebrospinal fluid primarily mediate an outside-in lesional gradient in the spinal cord. Taken together, this study provides support for long-term targeting of inflammatory demyelination in the spinal cord and nominates vascular dysfunction as a potential target for new therapeutic approaches to limit irreversible disability.

Immune Signature of Bronchiolitis Obliterans Syndrome after HCT Derived from Blood, Bronchoalveolar Lavage, and Tissue

Presenting Author: Williams, Kirsten, MD, Pediatric BMT

Poster Number: 27

Qayed, Muna; Pavletic, Steve; Holtzman, Noa; Hakim, Fran; Switchenko, Jeffrey; Rose, Jeremy; Gress, Ronald; Flomerfelt, Frank; Justus, David; Suffredini, Anthony; Farthing, Don; Rosenberg, Ari; Kleiner, David; Halter, Joerg; Tamm, Michael; Savic Prince,

Background: Bronchiolitis Obliterans Syndrome (BOS) is a rare complication of allogeneic hematopoietic cell transplant (HCT) with poor prognosis. We have previously linked leukotrienes and Th2 cells to progressive BOS, through investigations of bronchoalveolar lavage fluid (BAL), blood, urine, and clinical response to leukotriene blockade and others have shown MMP3 and osteopontin are higher in BOS vs. those with chronic graft versus host disease of other organs (cGVHD-BOS). We hypothesized that we could identify an immune signature of BOS, supporting a role for activated Th2 and alternatively activated macrophages.

Methods: Blood, BAL, and lung biopsies were obtained on IRB approved protocols. Plasma was compared between patients with BOS (n=39) and those with cGVHD-BOS (n=38), and healthy controls (HC, n=8), using protein array (Searchlight, acquired by Aushon Technologies), and Luminex assay. BAL was compared between those with BOS (n=16) and HC (n=4) using a protein Discovery Assay (Eve Technologies). Tissues were assayed using immunohistochemistry. BOS was diagnosed per 2014 consensus criteria, with active disease defined <2 years of cGVHD diagnosis.

Results: Serum osteopontin levels were significantly higher in BOS vs. GVHD-BOS (median 345,955 vs. 164,453 pg/mL, p=0.009) by protein array, with similar results by Luminex assay in a subset of samples with HC, p<0.05), and remained elevated when restricting to active disease. Osteopontin co-located with BOS lesions. MMP3 was not higher in the total cohort, but trended higher with active disease, 72,065 vs. 23,885, p=0,06). In BAL of nonresponding non-infected patients, IL-4, IL-23, CCL15 were elevated in BOS vs. HC, p<0.05.

Discussion: While limited by small numbers, our data confirm that osteopontin is a biomarker of BOS, and support that the source is the lung BOS lesions. Consistent with our prior finding that BOS BAL is enriched for TH2, IL-4, IL-23, and CCL15 were higher in BOS vs. HC BAL. Although not significant, elevated MMP3 in active but not the total cohort of BOS patients suggests that this may be a marker of active disease. Collectively our data support that BOS is driven by Th2/alternatively activated macrophage activation. Future studies are needed to validate these findings which could direct novel therapies.

Rapid Unpaired CBCT-Based Synthetic CT for CBCT-Guided Adaptive Radiotherapy

Presenting Author: Wynne, Jacob, M.D., Radiation Oncology

Poster Number: 28

Wynne, Jacob F.; Lei, Yang; Pan, Shaoyan; Wang, Tonghe; Pasha, Mosa; Luca, Kirk; Ropert, Justin; Patel, Pretesh; Patel, Saga A.; Godette, Karen; Jani, Ashesh B.; and Yang, Xiaofeng

Background: Quantitative cone beam CT (CBCT) is the foundation for image-guided radiation therapy, improving treatment setup, tumor delineation and dose calculation, but suffers from severe artifacts. Deep learning can overcome these , boosting quality critical for online adaptive radiotherapy (ART). Adapted contrastive unpaired translation (CUT), a recent method for image-to-image translation of photographic images, can improve CBCT quality while reducing compute time, demonstrating utility for ART.

Methods: CBCT and QACT images from 79 patients receiving proton therapy for prostate cancer 2019 - 2020 were retrospectively collected. QACT images were acquired in accordance with institutional policy. 79 patients yielded 102 image sets. CBCT images were shuffled for unsupervised training and QACT-quality synthetic CT images were generated as outputs. Mean absolute error (MAE), structural similarity index measure (SSIM), and Fréchet inception distance (FID) were compared against same-day QACT.

Results: MAE, SSIM, and FID were compared for the CycleGAN and CUT data relative to input QACT and are reported as the mean across five-fold cross-validation ± standard error. CUT achieved superior performance in MAE (19.5 ± 3.9 HU vs. cycleGAN 47.1 ± 25.4) and FID (31.5 ± 6.6 vs cycleGAN 75.9 ± 41.3). MAE indicates pixel-level correspondence to QACT HU intensity values,

making the synthetic outputs of CUT useful for dose calculations during ART. FID further demonstrates perceptual visual similarity. SSIM for CycleGAN (0.7 ± 0.2) and CUT (0.8 ± 0.0) were similar, indicating acceptable reproducibility of global structure.CUT was faster and lighter than CycleGAN. CycleGAN contained a total of 28,286,000 parameters; CUT contained 14,703,000, approximately half that of CycleGAN. As a result, CycleGAN computes on a single CT image slice over 0.33s while CUT requires just 0.18s.

Conclusion: The contrastive method investigated here was demonstrated to be faster and more accurate than CycleGAN, requiring fewer networks and parameters to achieve superior performance. We demonstrated anatomic boundary preservation and HU fidelity superior to cycleGAN while significantly reducing compute time. We plan to investigate the use of these synthetic CT images in automated segmentation prior to exploration of CUT in a prospective setting.

IgM Drives the CD4 T Cell Response to Factor VIII in Mice

Presenting Author: Zerra, Patricia, MD, Pathology and Laboratory Medicine

Poster Number: 29

ZERRA, PATRICIA E; McCoy, James W; Patel, Seema R; Kim, Sungwoong; Arthur, Connie; Fuller, Megan; Kalman, Dan; Baafi, Deborah; Clark, Tarralyn; Hakim, Sahl; Baldwin, W Hunter; Parker, Ernest; Meeks, Shannon; and Stowell, Sean R

BACKGROUND: Despite new treatment options, the development of anti-factor VIII (FVIII) antibodies, or inhibitors, continues to limit optimal therapy options for patients with hemophilia A. No prophylactic strategy exists that can actively prevent inhibitor formation, largely stemming from a lack of understanding regarding key initiating immune pathways. In contrast to other model antigens, inhibitor formation occurs only following multiple FVIII exposures, suggesting that early exposure events may prime subsequent development of long-lasting antibodies. Improved understanding of the timing and factors influencing CD4+T cell activation is necessary for the development of strategies to prevent antibody formation.

METHODS: Mice lacking B cells, unable to secrete IgM (IgMsd), defective in marginal zone (MZ) B cell trafficking (S1PR1TSS), or hemophilia A mice received 1-3 weekly exposures to FVIII +/- CD4+T cell or MZ B cell depletion. FVIII-OVA and a FVIII-specific CD4+T cell tetramer were used to assess T cell proliferation following FVIII exposure +/- MZ B cell depletion or passive administration of anti-FVIII IgM. Anti-FVIII IgM and IgG was examined by enzyme-linked immunoassay.

RESULTS: Recipients receiving 1-2 FVIII exposures produced anti-FVIII IgM alone. In comparison, recipients with 3 exposures additionally generated anti-FVIII IgG. CD4+T cell proliferation significantly increased following the 3rd FVIII exposure. Proliferation was significantly impaired in B cell-deficient recipients and in mice lacking MZ B cells, with an absence of anti-FVIII IgM and IgG. S1PR1TSS recipients developed anti-FVIII IgG at comparable levels to controls. IgMsd recipients receiving FVIII

had a blunted IgG response and absent CD4+T cell proliferation. Exposure of a FVIII-naïve recipient to IgM anti-FVIII induced robust OTII proliferation after only 1 FVIII exposure. Thus, IgM antibodies alone converted a recipient from a state of CD4+T cell non-responsiveness to robust proliferation.

CONCLUSION: Our findings suggest an unexpected mechanism of CD4+T cell activation following FVIII exposure. We hypothesize that early FVIII exposure results in MZ B cell generation of an IgM response that induces CD4+T cell proliferation and the generation of anti-FVIII IgG following 3 exposures to FVIII. Targeted approaches to prevent anti-FVIII antibody formation may be most effectively achieved by defining key factors regulating early IgM formation following initial FVIII exposure.

Orthostatic hypotension symptoms and cardiac interoception – an interplay of physiology, cognition, and interoceptive beliefs.

Presenting Author: Beach, Paul, D.O., Ph.D., Neurology

Poster Number: 30

Beach, Paul; McCallister, Brady; Leightheiser, Grace; Kim, Michelle; Gibbons, Christopher; and Freeman, Roy

Over 50% of patients with orthostatic hypotension (OH) from autonomic failure have no postural symptoms. Interoception, the neural processing and/or awareness of internal states, may be disrupted by autonomic neuropathology. We hypothesized that absent OH symptoms are a manifestation of impaired interoception.

Participants with OH (N=32; 11 females; mean age 67.3 years) underwent seated, computer-based cardiac interoceptive testing (Cardioception). All performed and provided confidence ratings for a heartbeat counting (HBC) task. A subset (N=20) completed a psychophysical heartbeat discrimination (HRD) task, allowing quantification of accuracy, bias (error between truth and perception), precision (variance of bias), and confidence for heart rate (interoceptive) and auditory (exteroceptive) tasks. Orthostatic responses (heart rate/HR, systolic blood pressure/SBP) were then measured during a 5-minute head-up tilt test. A structured interview assessed orthostatic symptoms (Q1 of the OH Questionnaire (OHQ)). Montreal Cognitive Assessment (MoCA) screened cognition. Maximum tilt-induced OHQ1 scores of <3 delineated groups ('symptomatic' or 'non-symptomatic'). Separate binomial logistic regressions tested associations between symptom status and 1) clinical variables, 2) HBC performance/confidence, and 3) interoceptive and exteroceptive HRD metrics. Spearman correlations were calculated across individuals, and after group stratification, between symptom scores, cardioception metrics, MoCA, and orthostatic vitals. Significance levels were: $p<0.01$ (stratified correlations) and otherwise $p<0.05$.

Non-symptomatic patients (N=18) had a lower supine HR (Wald=5.6, p=0.02) and higher SBP (Wald=3.9, p=0.05) than symptomatic individuals. The non-symptomatic group had greater HBC accuracy, compared to the symptomatic group (Wald=4.7, p=0.03), with a similar trend for HRD interoceptive accuracy (Wald 3.4, p=0.066). OHQ scores tended to be negatively correlated with HBC accuracy across individuals (HBC rho=-0.35, p=0.05). Lowest tilt SBP broadly correlated with HBC confidence (rho=0.51, p=0.003) and negatively with interoceptive precision (rho=-0.49, p=0.03). MoCA correlated with HBC accuracy (rho=0.39, p=0.03), a result driven by symptomatic individuals (rho=0.71, p=0.005). Group-stratified correlations in non-symptomatic individuals additionally found negative relationships between lowest tilt SBP and HBC accuracy (rho=-0.55, p=0.003) and between MoCA and interoceptive bias (rho=-0.78, p=0.003).

This pilot study found that OH symptom report inversely associated with aspects of cardioception, which correlated with some orthostatic measures. However, cognitive status and interoceptive beliefs are likely additional influences on this relationship.

Activity Assessment of Factor Replacement Therapies to Guide Infusion Rate Protocols in Patients with Bleeding Disorders

Presenting Author: Choe, Yeon-Whan, DO, Pathology

Poster Number: 31

CHOE, YEON-WHAN; Grewal, Sarah K.; DiGiandomenico, Stefanie; Hanson, Laura; Barrette, Eileen; Then, Caroline; Carver, Newton; and Maier, Cheryl L.

Background: Inclusion of new factor products on formulary at our institution raised consideration for optimal administration routes, including whether a bolus intravenous push versus infusion over 4-12h provided acceptable factor activity. Here we assessed the activity of two clotting factor replacement therapies over a 24h period to guide clinical care protocols.

Method: Two vials each of Novoeight and Vonvendi were reconstituted to clinically relevant potencies (13 IU/ml, Novoeight; 27 IU/ml, Vonvendi). Products were spiked separately into factor VIII-deficient plasma (Novoeight) or assay diluent (Vonvendi), and tested for activity at various timepoints. Novoeight samples were assessed by traditional one-stage FVIII assays, while Vonvendi samples were assessed for VWF antigen, ristocetin cofactor activity (RCA), and glycoprotein Ib binding activity (GP1bM).

Results: Novoeight samples maintained similar FVIII activities at all timepoints tested, with differences falling within the coefficient of variation of the assay. Specifically, the two samples had FVIII levels of 108% and 95% at baseline and levels of 98% and 91%, respectively, at 12h, which was the timepoint of greatest interest given plans to allow 12h infusion rates. For Vonvendi samples, measurement of VWF antigen remained fairly stable throughout the 24h period. However, VWF activity decreased in both RCA and GP1bM assays over time, including by 4h. RCA values were 193% and 190% at baseline, 113% and 95% at 4h, and 63% and 63% at 12h. GP1bM was 140% and 133% at baseline, 92% and 91% at 4h, and 56% and 70% at 12h. Together, these results supported implementation of protocols allowing for extended (up to 12h) infusion of Novoeight and short (3-5min) bolus infusion of Vonvendi.

Conclusion: Our study demonstrated maintained Novoeight activity over the study period, confirming infusion rates of 12h should be efficacious. Conversely, Vonvendi yielded significantly decreased activity levels in as little as 4h, indicating the need for faster infusion rates. Based on our results, current practices at our institution were adapted to include extended infusion only for Novoeight. The clinical lab should continue to play a primary role in testing and developing patient care protocols for therapeutic drugs through multidisciplinary collaboration.

The beneficial microbe, Lactococcus lactis subspecies cremoris, drives prevention of metabolic disease and hepatoprotection via rewiring of metabolic pathways in the gut and liver

Presenting Author: Gacasan, Camilo Anthony, BS, Pediatrics

Poster Number: 33

Gacasan, C. Anthony; Weinberg, Jaclyn; Naudin, Crystal; Askew, Lauren; Barbia, Stefi; Jones, Dean; and Jones, Rheinallt

Background: With over two-thirds of US adults either overweight and obese and one-fifth of US children aged 2-19 years, the prevalence and comorbidity associated with metabolic syndrome are of significant consequence to the US population. Dietary supplementation with beneficial microbes may be an integral tool to add to our therapeutic toolbox to mitigate the comorbidity associated with increased weight. Our research group has previously identified the microbe Lactococcus lactis subspecies cremoris (LLC) as a highly efficacious probiotic in the attenuation of western style diet induced metabolic syndrome phenotypes and through the utilization of ultra-high performance liquid chromatography (UHPLC-HRMS) coupled to high resolution mass spectrometry we show that this may be in part due to changes in gut-derived small molecules.

Methods: C57BL/6 mice were fed a western style high fat, high carbohydrate diet and were supplemented with 1x109 colony-forming units of LLC (ATCC 19257), Lactococcus lactis Rhamnosus GG (LGG) as a control bacteria (ATCC 53103), or an HBSS vehicle control 3 times per week for 16 weeks to assess for effects on long term metabolic outcomes. Small molecule metabolomic analysis was conducted on the serum of mice treated with western style diet supplemented with the same probiotic experimental groups for 4 weeks, metabolites measured via UHPLC-HRMS and analyzed with publicly available computational tools and functional pathway enrichment algorithms.

Results: Mice fed a western style diet supplemented with LLC gained less weight, developed less hepatic inflammation and steatosis, and lower overall cholesterol levels than mice fed control bacteria. LLC fed mice showed a discrete population of serum metabolites when compared to either vehicle or control bacteria and demonstrated functional enrichment in pathways related to fatty acid metabolism and activation and cholesterol metabolism.

Conclusions: LLC is a highly efficacious probiotic that when supplemented in the context of a high fat and high carbohydrate diet in mice results in a distinct population of gut derived changes in serum and liver metabolites that may be driving the decreased weight gain, decreased liver adiposity and inflammation, and reductions in serum cholesterol we observed.

Implementing an Enhanced Recovery Protocol with Automated Data Display and Statistical Process Control Analysis: A Quality Improvement Initiative

Presenting Author: Galloway, James, MD, Surgery

Poster Number: 34

Galloway, J. Luke; Powell, Krista M.; Pollock, Jonathan D.; Massarweh, Nader N.

Background: The 2022 Veterans Affairs National Surgery Office (NSO) Annual Surgery Report indicates length of stay after colectomy in Veterans Health Administration (VHA) surgery programs is 8.5 days. Enhanced Recovery After Surgery (ERAS) protocols are associated with shortened length of stay and improved outcomes when applied to patients who undergo colorectal surgery. While facility-specific approaches have been recommended, the optimal method for developing and implementing ERAS protocols as a quality improvement initiative has not been characterized. We hypothesized automated data collection from the Corporate Data Warehouse (CDW) and statistical process control (SPC) methods could provide data-driven insights necessary for successful ERAS implementation and ongoing quality improvement.

Methods: We developed a CDW query and automated data display for our defined surgical population from October 2021 to November 2023 which was analyzed at regular intervals using SPC. These data were reviewed monthly by an interprofessional team who concomitantly participated in iterative updates to a facility-specific ERAS protocol. Compliance with protocol elements was monitored by chart review and similarly analyzed with SPC.

Results: Our query provided automated data collection for our defined population of 91 colorectal surgery patients. SPC analysis of post-operative length of stay revealed widely variable processes with a mean of 7.3 days (±8.0 days), range of 52 days (2-54 days), and 7 signals of special cause variation. All improved over the course of 9 months to a mean of 5.8 days (±4.6 days), range of 23 days (2-25 days), and 2 signals of special cause variation. SPC analysis of protocol compliance revealed improvement from 0% to 67%.

Conclusions: Automated data collection from CDW and SPC analysis can provide data-driven insights into the development, implementation, and evaluation of ERAS protocols which can be used by clinical teams as quality improvement initiatives. These tools can be broadly applied to encourage continuous process improvement and interprofessional collaboration.

Evaluation of Flow Cytometry Utility in Hematopoietic Progenitor Cell Products for Patients with Multiple Myeloma Undergoing Stem Cell Collection

Presenting Author: Grewal, Sarah K, DO, MPH, Department of Pathology and Laboratory Medicine

Poster Number: 35

GREWAL, SARAH K; Javanbakht, Ayda; Yee, Marianne; Hendrickson, Jeanne; Waller, Edmund K.; and Sullivan, H. Cliff

Peripheral blood stem cell (PBSC) collection plays a pivotal role in the therapeutic paradigm for multiple myeloma (MM). While current regulations address essential components such as sterility,

viability, and cell count, collection and processing practices among institutions vary. For example, evaluation of persistent disease is not mandated but some laboratories perform flow cytometry on human progenitor cell apheresis (HPCA) products. Here, our goal is to assess the clinical benefit of this extra testing in guaranteeing the quality of PBSC collections for MM patients. A retrospective chart review was done for patients with MM who had autologous stem cell collections from October 2022 through January 2024. Data extracted included flow cytometry results for HPCA products, pre-transplant and post-transplant bone marrow (BM) biopsies, and date of stem cell transplant, if applicable. Flow cytometry results were reported as percent clonal plasma cells based on signed hematopathology reports of the leukemia/lymphoma panel using markers for CD19, CD27, CD38, CD45, CD56, CD81, CD117, CD138, KAPPA (cytoplasmic), and LAMBDA (cytoplasmic). Values were categorized as 0%, <1%, or >1%. The Fisher's Exact test (SAS v9.4; Cary, NC) was used to compare results. Of 354 patients with HPCA products, six (1.7%) had positive flow cytometry results, all <1%. Within the cohort, 109 patients (31%) had positive pre-transplant BM biopsy results, with clonal cell values ranging from <1% to 63%. On average, pre-transplant BM biopsies were done 25 days before the date of collection (median 15), and 47 days before transplant (median 31). 183 patients had post-transplant data available. 1 of 6 positive HPCA products had a post-transplant result, which was negative. Additionally, 21 cases (11.5%) displayed low levels (<1%) of clonal cells post-transplant, despite a negative HPCA product result. All positive HPCA products had positive pre-transplant results, while 69% of negative HPCA products had negative pre-transplant results. Of note, none of the negative pre-transplant flow results had a positive HPCA product result. Based on these results, under 2% of patients demonstrated minimal residual disease in the HPCA product, indicating test overutilization of flow cytometry in the evaluation of MM patients.

Toward a generalizable machine learning workflow for neurodegenerative disease staging with focus on neurofibrillary tangles

Presenting Author: Gutman, David, MD PhD, Pathology

Poster Number: 36

GUTMAN, DAVID; Vizcarra, Juan Carlos; Pearce, Thomas; Dugger, Brittany; Keiser, Michael; Gearing, Marla; and Glass, Jonathan

Machine learning (ML) has increasingly been used to assist and expand current practices in neuropathology. However, generating large imaging datasets with quality labels is challenging in fields which demand high levels of expertise. Further complicating matters is the often seen disagreement between experts in neuropathology-related tasks, both at the case level and at a more granular level. Neurofibrillary tangles (NFTs) are a hallmark pathological feature of Alzheimer disease, and are associated with disease progression which warrants further investigation and granular quantification at a scale not currently accessible in routine human assessment. In this work, we first provide a baseline of annotator/rater agreement for the tasks of Braak NFT staging between experts and NFT detection using both experts and novices in neuropathology. We use a whole-slide-image

(WSI) cohort of neuropathology cases from Emory University Hospital immunohistochemically stained for Tau. We develop a workflow for gathering annotations of the early stage formation of NFTs (Pre-NFTs) and mature intracellular (iNFTs) and show ML models can be trained to learn annotator nuances for the task of NFT detection in WSIs. We utilize a model-assisted-labeling approach and demonstrate ML models can be used to aid in labeling large datasets efficiently. We also show these models can be used to extract case-level features, which predict Braak NFT stages comparable to expert human raters, and do so at scale. This study provides a generalizable workflow for various pathology and related fields, and also provides a technique for accomplishing a high-level neuropathology task with limited human annotations.

Complications of Delayed Ureter Reconstruction following Traumatic Ureter Injury

Presenting Author: Hart, Lucy, MD, General Surgery

Poster Number: 37

Hart, Lucy; Williams, Sonya; Hanos, Dustin; Roorbach, Madeline; De Leon Castro, Luis; Grady, Zachary; Smith, Randi; Nguyen, Jonathan; Sciarretta, Jason

Background: Traumatic ureter injuries (TUI) are infrequently encountered and difficult to manage. For TUI requiring open repair, management decisions regarding reconstruction timing often varies: some patients may undergo immediate or early ureter repair, while some may require urinary diversion followed by eventual repair weeks later. Our primary aim is to compare infectious complications for early vs. delayed TUI repair. We hypothesized that patients requiring delayed repairs experience higher rates of infectious complications.

Methods: A retrospective review of all TUI in adult patients was conducted at a high volume Level I trauma center from October 2011-2023. Delayed ureter reconstruction was defined as those repaired >7 days after TUI.

Results: A total of 106 ureter injuries were identified, 59 of which required operative repair. All were the result of penetrating injury. Forty-eight (81.4%) underwent early repair at a mean 1.4 days after TUI, while 11 (18.6%) had late repairs at a mean 223 days. Delayed repair was associated with higher rates of damage control laparotomy (63.6% vs. 29.2% p=0.31), although injury severity score, and admission vitals and labs were similar between the two groups.

Delayed TUI repair was associated with a higher risk of urinary tract infection (UTI) (90.9% vs. 33.3% p<0.001), recurrent UTI (54.5% vs. 2.1% p<0.001), and percutaneous nephrostomy tube (PCN) dislodgement (p<0.001). Delayed repair was also with loss of renal function requiring nephrectomy or indefinite PCN (36.4%vs. 6.3% p=0.005).

Conclusion: Intraoperative instability often necessitates delayed TUI repair with initial damage-control ureteral management, followed by eventual reconstruction. Patients undergoing delayed repairs have

higher rates of UTI and loss of renal function when compared to those repaired early. Ureter repair during index operation or early takeback may mitigate these complications.

Structural Basis of Multiprotein Recognition by the P. aeruginosa Outer Membrane Protein OprM

Presenting Author: Henes, Mina, MD/PhD, BCDB

Poster Number: 38

Henes, Mina; and Conn, Graeme

Pseudomonas aeruginosa is a growing threat to the healthcare system, especially to immunocompromised patients, with infections that are challenging to treat due to intrinsic resistance to many clinically relevant antibiotics. Expression of multiple members of the Resistance-Nodulation-cell Division (RND) superfamily of multidrug efflux pumps contributes significantly to this intrinsic resistance. RND efflux systems are tripartite protein complexes, e.g. MexAB-OprM, comprising an inner membrane-embedded transporter protein (e.g. MexB), a periplasmic adaptor protein (PAP; e.g. MexA) and an outer membrane factor (OMF; e.g. OprM). OprM forms functional complexes with different PAPs, including MexA and MexX, whereas other OMFs, such as OprJ and OprN, have single, specific partners. The basis of this specificity or promiscuity in PAP/OMF interaction is currently not known. Using published crystal structures, cryoEM structures, and homology models, this work has three goals: (1) establish an appropriate molecular dynamics (MD) simulation protocol for membrane-embedded PAP/OMF complexes, (2) develop the computational tools to analyze these simulations, and (3) use these procedures to simulate individual OMFs and their complexes with PAPs to define the basis of OMF selection in RND efflux pump assembly. Energy plots from MD simulations show that we successfully developed a protocol for membrane-bound proteins. All systems were simulated using this protocol and the analysis program is currently in development and publicly available through GitHub. While outer membrane fusion proteins share a high sequence similarity, initial results suggest that differences in protein conformation and electrostatic landscape contribute to the observed differences in OMF interacting partner selectivity.

The Relationship between Childhood Trauma and Negative Symptom Severity in Patients with Schizophrenia who have Elevated CRP

Presenting Author: Jones, Mackenzie, MD MPH, Department of Psychiatry

Poster Number: 39

JONES, MACKENZIE T.; Miller, Andrew H.; Goldsmith, David R.

BACKGROUND: Childhood trauma has independently been linked to an increased risk of schizophrenia as well as increased inflammation. Inflammation has been linked to negative symptoms

involving motivation and pleasure in schizophrenia. We hypothesized that there would be an association between inflammation, childhood trauma and negative symptoms.

METHODS: Data was collected from 57 patients with schizophrenia who were recruited from the outpatient behavioral health clinics at Grady Hospital. Subjects underwent blood sampling for inflammatory markers including hsCRP and a panel of cytokines. Subjects were administered the Childhood Trauma Questionnaire (CTQ) to assess history of childhood trauma and the Brief Negative Symptoms Scale (BNSS) to assess the severity of their negative symptoms. We ran bivariate non-parametric correlations on the associations between the CTQ, BNSS, and inflammatory markers.

RESULTS: Emotional Neglect (rT =.212, p = .026) and Physical Neglect (rT =.210, p=.031) subscales of the CTQ were positively correlated with the Motivation and Pleasure Dimension (MAP) of the Brief Negative Symptoms Scale (BNSS), but not the Emotional Expressivity (EXP) Dimension. hsCRP was positively correlated with BNSS MAP (r=.352, p=.007), but not BNSS EXP. In the group as a whole, there was no significant relationship between CRP and CTQ. When divided into groups of low, moderate, or high concentrations of hsCRP (N=12, 26, 19 respectively), subjects with high (>3mg/L) concentrations of hsCRP, showed significant associations between Emotional Neglect (rT = .463, p = .008) and Physical Neglect (rT = .365, p = .040) with BNSS MAP, which were not found in subjects with low (<1mg/L) or moderate (1-3mg/L) concentrations of hsCRP. Additionally, we created an interaction term for CRP and combined scores of Emotional and Physical Neglect and found a significant relationship with BNSS MAP (rT =.301, p = .008).

CONCLUSIONS: A history of childhood emotional and physical neglect is associated with the severity of negative symptoms related to motivation and pleasure in patients with schizophrenia, a finding only seen in patients with high inflammation. Future studies should consider enriching for patients with these factors (i.e., childhood trauma, high inflammation, and high deficits in motivation and pleasure) in treatment trials using anti-inflammatory approaches.

Improving the Utility of a Cancer Gene Mutation Panel for Multiple Myeloma Patients

Presenting Author: Patel, Lalit, MD, PhD, Pathology

Poster Number: 40

Patel, Lalit; Zhang, Linsheng; Smith, Geoff H; Schneider, Thomas; Jaye, David

Background: Multiple myeloma (MM) is a plasma cell malignancy that is initiated by chromosomal instability and rearrangement, with >90% of cases demonstrating clonal cytogenetic abnormalities. Classification and consensus guidelines therefore categorize MM using ploidy and chromosomal abnormalities. Interestingly, a portion of Emory's test volume for our 75-gene mutation panel (MMP75) is for MM cases. This suggests the test is utilized for purposes other than diagnostic workup.

Methods: Anecdotes were obtained from ordering physicians regarding their use of MMP75 and a formal survey is underway to assess how the results of MMP75 testing were used: to inform diagnosis,

determine prognosis, guide treatment, explain progression, identify/rule-out secondary neoplasia, or no effect on management. To gauge suitability of MMP75 for these purposes, a retrospective analysis was performed on variants identified from testing the bone marrow of patients who received cytogenetic workup for MM between 2019-2024.

Results: Anecdotes from ordering physicians suggest an interest in MMP75 when informing prognosis, selecting treatments, and evaluating for treatment associated secondary neoplasms. Retrospective analysis found the number of pathogenic variants ranged from 1-8/case with mutations detected across 42 genes. The genes most frequently identified with pathogenic mutations were TP53 (22.4%), DNMT3A (19.2%), TET2 (14.7%), and ASXL1 (12.2%). All four are associated with poor prognosis in MM. Events in therapeutic targets include mutations activating RAS/RAF (16.7%), JAK/STAT (2.6%), and KIT (0.6%) signaling.

Conclusions: MMP75 detects mutations relevant to patients with MM. However, the variants are not unique to MM. DNMT3A, TET2, and ASXL1 mutations occur in clonal hematopoiesis (CHIP) and various myeloid neoplasms. TP53 mutations and activating RAS/RAF, JAK/STAT, and KIT variants occur in various hematologic malignancies. This encumbers distinguishing whether variants inform on a patient's MM or suggesting a secondary neoplasm. Future work will evaluate the effect of enriching plasma cells in repeat testing on variant allele frequency (VAF) as a metric that may address this limitation.

Transversus Abdominis Plane (TAP) Block for Children with Sickle Cell Disease Undergoing Elective Surgery.

Presenting Author: Raikot, Swathi, MBBS, Pediatric Surgery

Poster Number: 32

RAIKOT, SWATHI; Keane, Olivia; Dantes, Goeto; Harlan, Danielle; Trinidad, Jose María; He, Zhulin; Heiss, Kurt; Alemayehu, Hanna; and Santore, Matthew.

Background: Pediatric patients with sickle cell disease can have unique challenges with postoperative pain management. However, literature on postoperative pain control strategies in this population is sparse. This single-institutional retrospective study aimed to evaluate the impact of ultrasound-guided transversus abdominis plane (TAP) blocks on perioperative opioid requirement in pediatric patients with sickle cell disease undergoing elective surgeries such as open umbilical hernia repair (UHR) or laparoscopic cholecystectomy (CCY).

Methods: Patients ≤18 years of age with sickle cell disease who underwent either UHR or CCY with TAP block between September 2017 - 2022 were compared to those without TAP block during the same time period. Demographics, opioid use, length of stay (LOS), postoperative complications, and returns to the system were compared using Wilcoxon's rank sum test and Fisher's exact test. Opioid use was measured as Morphine Milligram Equivalents (MME).

Results: Of 158 patients, 54 underwent UHR and 104 underwent CCY. TAP blocks were performed in 35 (65%) UHR and 21 (20%) CCY. In the UHR group, patients who received TAP block had a lower median opioid prescription at discharge compared to those without a TAP block (median (IQR): 0 (0, 0.4) vs. 2.3 (0, 5) MME, p=0.002). Similarly, in the CCY group, the median perioperative opioid requirement was lower among those who received TAP block compared to those without a TAP block (median (IQR): 0 (0, 6.9) vs. (6 (1.8, 12) MME, p=0.017). Additionally, no patients with TAP block in the UHR group received acetaminophen postoperatively (0% vs. 20% in non-TAP block, p=0.04), with no difference in the use of other non-opioid pain medications (p>0.05). Furthermore, there was no difference in LOS, postoperative complications or returns to the system between those with and without TAP block in either of the surgical groups.

Conclusion: The use of ultrasound-guided transversus abdominis plane (TAP) blocks for postoperative pain control in pediatric patients with sickle cell disease was associated with decreased perioperative opioid exposure following laparoscopic cholecystectomy and decreased opioids at discharge following umbilical hernia repair without an increase in postoperative complications.

The Utility of Spectroscopic MRI in Stereotactic Biopsy and Radiotherapy Guidance in Newly Diagnosed Glioblastoma

Presenting Author: Rejimon, Abinand, Bachelor of Science, Emory School of Medicine

Poster Number: 19

Rejimon, Abinand; Ramesh, Karthik; Trivedi, Anuradha; Huang, Vicki; Schreibmann, Eduard; Weinberg, Brent; Kleinberg, Lawrence; Shu, Hui-Kuo; Shim, Hyunsuk; and Olson, Jeffrey

Background: Glioblastoma (GBM) prognosis remains poor despite aggressive treatment. Standard care involves surgery, radiation, and chemotherapy, but limitations persist. Spectroscopic MRI (sMRI) offers improved tumor characterization by measuring metabolite levels. Elevated Choline (Cho) and decreased N-acetylaspartate (NAA) indicate proliferating tumor cells not always detected in standard MRI. Our pilot study on GBM patients treated with belinostat and chemoradiation examines the link between undertreated tumor detected with sMRI and overall survival (OS). We also analyze recurrence patterns using volumetric analysis, hypothesizing that recurrence will appear in areas indicated by sMRI but not standard MRI.

Methods: Our retrospective analysis used data from 24 grade IV GBM patients (control: n = 12, belinostat: n = 12) from the NCT02137759 study. Cohorts were divided based on median difference between pre-radiotherapy sMRI and treated T1w Contrast Enhanced (T1w-CE) volume. High-Mismatch had greater sMRI vs. T1w-CE volume difference; Low-Mismatch had smaller. Kaplan-Meier estimator calculated median OS for each subgroup. Our recurrence analysis measured overlap between recurrence volume (rCE), pre-RT sMRI volume, and clinical treatment volume (CTV). Patients with rCE and CTV overlap >55% had in-field progression; <55% were out-of-field progression. Patients with rCE & sMRI overlap greater or less than 20% were quantified.

Results: The median OS was 14.4 months in the High-Mismatch group compared with 34.3 months in the Low-Mismatch group. The T1w-CE volumes were similar in both subgroups. See Figure 1. Our overlap analysis showed that the control cohort had 9/12 patients experience in-field progression compared to the belinostat cohort with 4/11. Additionally, we showed that half of the patients in both cohorts had rCE volumes overlap with pre-RT sMRI volumes. See Figure 2.

Conclusion: We find that patients who had lower volumes of undertreated tumor detected by spectroscopy had better survival outcomes. Our recurrence analysis demonstrated that undertreated tumor volumes undetected in standard imaging, but detected with EPSI, tend to overlap with future recurrence patterns, suggesting the vital need for new tools to guide GBM treatment in the clinic. Further, this analysis shows promise in spectroscopy-guided RT combined with a radiosensitizer like belinostat as well as in accurately delineating targets of stereotactic biopsies.

A 3D Bioengineered Model to Study Fontan-Associated Liver Disease

Presenting Author: Rezapourdamanab, Sarah, M.D., Biomedical Engineering

Poster Number: 41

REZAPOURDAMANAB, SARAH; Singh, Yamini; Jin, Linqi; Norton, Sophia; Salar Amoli, Mehdi; Romero, Rene; Bauser-Heaton, Holly D.; and Serpooshan, Vahid

Introduction: The Fontan procedure is performed in children with single ventricle physiology, and has led to excellent short-term palliation and survival rates but at the cost of long-term complications. Fontan-associated liver disease (FALD) results from altered hemodynamics after the Fontan procedure that result in elevated central venous pressures, chronic alterations in hepatic perfusion and resultant hepatic fibrosis. Improved understanding of FALD pathophysiology is challenged by the lack of experimental models. The current liver models, mainly comprised of 2D or suspension cultures of hepatic cells, lack biomimicry. This study presents a 3D bioprinted perfusable human liver model for the in vitro study of hepatic fibrosis in response to altered flow conditions in FALD patients.

Methods: Vascular 3D model of hepatic sinusoid was biofabricated using hybrid bioinks in two distinct peripheral layers and a central lumen. The outer layer was cast with hepatic cells (HepG2) encapsulated in a mixture of gelatin methacrylate (GelMA) and collagen type I. The inner layer consisted of hepatic stellate cells (HSCs) in GelMA. Human endothelial cells (ECs) were seeded onto the central lumen. 3D cellular constructs were cultured in vitro for four weeks in static (control) or dynamic conditions, by circulating the culture media at varying flow rates to simulate sinusoid pressure characteristic of healthy vs. disease state. Using Volcano system in cath lab, we invasively measured the pressure in mid-channel. Cell viability, proliferation, and maturation into functional liver tissue as well as tissue stiffness were evaluated via microindentation, flow hemodynamics assays, metabolomic assays, and immunohistochemistry analyses.

Results: Bioengineered liver constructs cultured under static and dynamic conditions demonstrated high cell viability and growth and full endothelialization of the sinusoid channel. HepG2 cells exhibited long-term function and maturation, forming clusters. Under FALD flow conditions, there were notable changes in EC-HepG2 cell morphology compared to dynamic flow in the healthy range, accompanied by reduced levels of functional markers.

Conclusion: This proof-of-principle study introduces an innovative and highly biomimetic 3D model of hepatic sinusoid, which can serve as a robust platform for in vitro investigations of complex cell-microenvironment interactions in the context of FALD as well as other hepatic disorders.

Minimally Invasive or Open Techniques for Inadequate Future Liver Remnant? A Model-Based Evaluation.

Presenting Author: Smith, Savannah, MD, Surgery

Poster Number: 42

Smith, Savannah; and Sarmiento, Juan

Background: Liver hypertrophy techniques are employed for patients requiring major hepatectomy with anticipated future liver remnant (FLR) < 30%. Associating Liver Partition and Portal Vein Ligation for Staged Hepatectomy (ALPPS) is an accepted hypertrophy method requiring two-stage laparotomy. To reduce morbidity, liver venous deprivation (LVD) was introduced as a minimally invasive alternative.

Methods: We built a probabilistic Markov model with embedded discrete event simulation to assess clinical and economic implications of ALPPS versus LVD for major hepatectomy with anticipated FLR < 30%. Median time to resection for LVD was 47 days, during which disease progression (8.9%) or death (2.4%) could occur. Without adequate hypertrophy post-LVD, salvage ALPPS was employed. ALPPS carried a median inter-stage hospital stay of 11 days, overall hospital stay of 24 days, successful resection rate of 91%. Both techniques had unique complication and mortality risks. Costs (2022 USD) were estimated from published literature and national databases. Primary outcomes included quality-adjusted life years (QALYs) in the first post-hypertrophy year, medical costs, and incremental cost-effectiveness ratios. We conducted sensitivity analyses to evaluate the robustness of our model to changes in input parameters.

Results: LVD was associated with 0.60 QALYs and $62,500; and ALPPS, 0.58 QALYs and $126,500. LVD was therefore preferred in the base case with reduced cost and increased QALY. In probabilistic sensitivity analyses (PSA), changing several variables over defined distributions, LVD was preferred in 99% of iterations due to lower costs; however, LVD consistently resulted in fewer completion hepatectomies from disease progression and death pending adequate hypertrophy. While LVD decreased costs, in 43% of iterations, LVD also decreased QALYs compared to ALPPS (Figure). If

LVD's time-to-hypertrophy maxed at 30 days, PSA yielded LVD as the preferred strategy in >90% of iterations, increasing QALYs and decreasing costs compared to ALPPS in all scenarios.

Conclusions: From a cost-effectiveness perspective, LVD is preferred, as ALPPS is associated with increased costs without clinically significant differences in QALY. However, if time to adequate hypertrophy were reduced or patient selection optimized with at least 90% of patients undergoing LVD completed curative hepatectomy, LVD would significantly substantially improve QALYs while still saving costs compared to ALPPS.

Adoptively Transferred Type-17 TILs Penetrate and Persist in Cholangiocarcinoma Tumors.

Presenting Author: Warren, Emilie, MD, General Surgery

Poster Number: 43

WARREN, EMILIE AK; Bennett, Frances J; Wittling, Megen C; Wyatt, Megan M; Oppat, Kailey M; Maithel, Shishir K; Paulos, Chrystal M; Lesinski, Gregory B

BACKGROUND: While one study has shown efficacy of mutation-specific CD4+ tumor-infiltrating lymphocytes (TILs) in cholangiocarcinoma (CCA), the methods that yield T cell products with optimal function & phenotype still need refinement. Besides antigen specificity, the ability of transferred T cells to persist in vivo is crucial. We have shown that TILs polarized to type-17 phenotype exhibit effector- and stem-memory properties; thus, we hypothesize they will regress CCA and persist in vivo.

METHODS: Intrahepatic tumors were established in C57BL/6 mice by orthotopic injection of murine CCA line URCCA4.3 (KRASG12D,Trp53-/-). After 2 weeks, immune cells were isolated from digested tumors using CD45 selection. T cells were then expanded in culture under type-17 culture conditions: IL-2/6/21/β and CD3/ICOS agonist. In a separate cohort of lymphocyte-deficient mice, luciferase-expressing URCCA4.3 intrahepatic tumors were established. Mice preconditioned with 3 Gy total-body irradiation (TBI) were infused with 2.5x106 type-17 TILs. Tumor size was measured weekly via bioluminescence. Cheek bleed on day 7 post-ACT assessed presence of circulating T cells. On day 32, peripheral blood, spleens, lymph nodes (LNs) and tumors were harvested and processed for flow cytometry.

RESULTS: Post-expansion, >80% of TILs were CD8+, expressed type-17 transcription factor RORγt, and exhibited activated effector phenotype (CD69+CD44+CD62L-). IL-17 was low in the CD8+ subset (3.4%) but higher in CD4+ (7.4%). Compared to untreated animals, mice receiving ACT had reduced tumor growth rate over 14 days. These animals had T cells detected in blood 7 days after ACT, majority effector memory CD8+ T cells. By day 21, however, these tumors rebounded to similar size as untreated. At endpoint, T cells were present in all harvested tissues of ACT-treated mice. When examining distribution of T cell subsets, a greater proportion of total CD8s penetrated tumor. Intratumoral CD4 and CD8 T cells were exhausted, expressing CD39 (87%, 97% respectively) and PD-1 (82%, 68%), and there were fewer effector memory cells (14%, 2%).

CONCLUSIONS: This work shows that TIL expansion from CCA tumors is feasible and infused TIL can reach tumor & persist. Future efforts will modify TIL culture methods to maximize T cell functionality, while optimizing timing of ACT to achieve efficacy.

AI Models to Predict Generalized Anxiety Disorder from Gene Expression

Presenting Author: Williamson, Drew, MD, Pathology & Laboratory Medicine

Poster Number: 44

WISE, ANDREW; and Williamson, Drew

Background: Approximately 15 to 20% of adults in the United States suffer from anxiety in a given year [1]. Despite the high prevalence of generalized anxiety disorder (GAD), biomarkers for the condition have not been previously identified, hampering efforts at study of response to treatment due to subjectivity. Simultaneously, over the past several decades, there has been mounting evidence that disorders such as GAD, once thought to exist entirely in the mind, have reproducible correlated biological phenomena, particularly changes to the immune system [2]. Though a causal relationship has not been elucidated, immune dysregulation has been repeatedly associated with GAD. We aim to develop an AI model that can classify patients according to GAD status by analysis of the patterns of gene expression in whole blood.

Methods: Using data collected from a prior study [3] that analyzed the gene expression patterns in whole blood of patients with and without GAD, we trained various AI models to do the binary classification task of GAD vs. non-GAD. Briefly, we condensed the number of transcripts available to the models from more than 12,000 to the N most relevant transcripts, where we let N be equal to 10, 20, and 30. We then split the data randomly into mutually exclusive train, validation, and test sets and tested AI models across a range of complexities from basic logistic regression to more complex multi-layer perceptrons.

Results: In our testing, we found no clear relationship between number of transcripts available to the model and GAD prediction accuracy and no clear relationship between model complexity (including number of parameters) and GAD prediction accuracy. Our results are summarized in Table 1.

Conclusions: Over the range of transcript numbers and models tested, accuracies were fair to poor, implying a weak association between gene expression in whole blood and GAD status, at least under these experimental conditions. Future work will be done to refine the method for transcript selection, to test other AI models, and to gather other datasets to test how generalizable our models are.

Citations: [1]: Terlizzi, Emily P., and Maria A. Villarroel. Symptoms of generalized anxiety disorder among adults: United States, 2019. US Department of Health and Human Services, Centers for Disease Control and Prevention, National Center for Health Statistics, 2020.

[2]: Costello, Harry, et al. "Systematic review and meta-analysis of the association between peripheral inflammatory cytokines and generalised anxiety disorder." BMJ open 9.7 (2019): e027925.

[3]: Wingo, Aliza P., and Greg Gibson. "Blood gene expression profiles suggest altered immune function associated with symptoms of generalized anxiety disorder." Brain, behavior, and immunity 43 (2015): 184-191.

Author Index